JAERI-M
85-063

X-RAY PHOTOELECTRON AND X-RAY-INDUCED AUGER ELECTRON SPECTROSCOPIC DATA, III
—GRAPHITE, Si, SiC, Si_3N_4 and SiO_2—

June 1985

Teikichi A. SASAKI and Yuji BABA

日 本 原 子 力 研 究 所
Japan Atomic Energy Research Institute

JAERI-M レポートは，日本原子力研究所が不定期に公刊している研究報告書です。
入手の問合わせは，日本原子力研究所技術情報部情報資料課（〒319－11 茨城県那珂郡東海村）あて，お申しこしください。なお，このほかに財団法人原子力弘済会資料センター（〒319-11 茨城県那珂郡東海村日本原子力研究所内）で複写による実費頒布をおこなっております。

JAERI-M reports are issued irregularly.
Inquiries about availability of the reports should be addressed to Information Division, Department of Technical Information, Japan Atomic Energy Research Institute, Tokai-mura, Naka-gun, Ibaraki-ken 319-11, Japan.

© Japan Atomic Energy Research Institute, 1985

編集兼発行　日本原子力研究所
印　　　刷　山田軽印刷所

X-RAY PHOTOELECTRON AND X-RAY-INDUCED AUGER ELECTRON SPECTROSCOPIC DATA, III —— GRAPHITE, Si, SiC, Si_3N_4 and SiO_2 ——

Teikichi A. SASAKI and Yuji BABA

Department of Chemistry, Tokai Research Establishment, JAERI

(Received May 1, 1985)

The intrinsic data of the X-ray photoelectron spectra(XPS) including valence-band region and X-ray-induced Auger electron spectra(XAES) are presented for graphite, Si, SiC, Si_3N_4 and SiO_2. Soft ion-etching subsequently performed after heating at 350 °C under high vacuum was employed for removing adsorbates on the sample surface. Chemically clean surfaces were easily obtained by etching with 8 keV Ar^+-ion beam of ca. 4 $\mu A/cm^2$, and chemical shifts of Si2p line were determined to be 0.9 eV for the carbide, 2.1 eV for the nitride and 4.0 eV for the oxide. Using the data obtained in the present work, chemical states of the surfaces exposed to H_2^+ ions were studied. The observations suggest formations of C-H bonds on graphite and SiC surfaces, and Si-H bonds on Si, Si_3N_4 and SiO_2 surfaces, respectively.

Keywords: X-ray Photoelectron Spectroscopy, X-ray-induced Auger Electron Spectrocopy, Graphite, Si, SiC, Si_3N_4, SiO_2, Hydrogen Ion, Hydrogen Recycling, Hydride

X線光電子及びX線励起オージェ電子スペクトルデータ・III
ーグラファイト，Si，SiC，Si_3N_4及びSiO_2 ー

日本原子力研究所東海研究所化学部
佐々木　貞吉・馬場　祐治

（1985年5月1日受理）

グラファイト，Si，SiC，Si_3N_4，SiO_2について，X線光電子（XPS）スペクトル及びX線励起オージェ電子（XAES）スペクトルを測定した。表面吸着物質の除去は，350°Cの高真空加熱とイオンエッチングの併用により行った。試料の化学的清浄表面は4$\mu A/cm^2$の8keV Ar^+イオンビームでエッチングすることにより得られ，SiC，Si_3N_4，SiO_2に対するSi 2p線の化学シフトは，それぞれ0.9eV，2.1eV，4.0eVと決定された。本研究で得られたデータを用いて水素イオン照射表面の化学状態を解析したところ，グラファイト及びSiC表面ではC－H結合が，また，Si，Si_3N_4及びSiO_2表面ではSi－H結合が形成されたことを示唆する結果が得られた。

CONTENTS

1. Introduction 1
2. Experimental 1
  2.1 Materials 1
  2.2 Spectral measurements 2
3. Results and discussion 2
REFERENCES 5

目　　次

1. 序 1
2. 実　験 1
  2.1 材　料 1
  2.2 スペクトル測定 2
3. 結果と考察 2
参考文献 5

LIST OF TABLES

Table 1 Binding energies and chemical shifts of core lines. The values in parentheses are determined by accumulating signals from adsorbates for long period of time.

Table 2 Kinetic energies and chemical shifts of the Si(LVV) and Si(KLL) XAES lines.

Table 3 Loss energies of core-line photoelectrons.

Table 4 Peak intensity ratios of C1s/Si2s for SiC, N1s/Si2s for Si_3N_4 and O1s/Si2s for SiO_2. Calculated values are estimated by use of Scofield's cross-section.

LIST OF FIGURES

Fig. 1 XPS wide scan of graphite.
Fig. 2 C1s XPS spectrum of graphite.
Fig. 3 Valence-band XPS spectrum of graphite.
Fig. 4 C(KLL) XAES spectrum of graphite.
Fig. 5 XPS wide scan of Si.
Fig. 6 Si2p XPS spectrum of Si.
Fig. 7 Si2s XPS spectrum of Si.
Fig. 8 Valence-band XPS spectrum of Si.
Fig. 9 Si(LVV) XAES spectrum of Si.
Fig. 10 Si(KLL) XAES spectrum of Si.
Fig. 11 XPS wide scan of SiC.
Fig. 12 Si2p XPS spectrum of SiC.
Fig. 13 Si2s XPS spectrum of SiC.
Fig. 14 C1s XPS spectrum of SiC.
Fig. 15 Valence-band XPS spectrum of SiC.
Fig. 16 Si(LVV) XAES spectrum of SiC.
Fig. 17 Si(KLL) XAES spectrum of SiC.
Fig. 18 XPS wide scan of Si_3N_4.
Fig. 19 Si2p XPS spectrum of Si_3N_4.
Fig. 20 Si2s XPS spectrum of Si_3N_4.
Fig. 21 N1s XPS spectrum of Si_3N_4.
Fig. 22 Valence-band XPS spectrum of Si_3N_4.
Fig. 23 Si(LVV) XAES spectrum of Si_3N_4.
Fig. 24 Si(KLL) XAES spectrum of Si_3N_4.
Fig. 25 XPS wide scan of SiO_2.
Fig. 26 Si2p XPS spectrum of SiO_2.
Fig. 27 Si2s XPS spectrum of SiO_2.
Fig. 28 O1s XPS spectrum of SiO_2.
Fig. 29 Valence-band XPS spectrum of SiO_2.
Fig. 30 Si(LVV) XAES spectrum of SiO_2.
Fig. 31 Si(KLL) XAES spectrum of SiO_2.
Fig. 32 Changes in C/Si ratio of SiC as functions of hydrogen fluence and Ar^+ ion fluence. AES data were determined from signal ratios of Si(LVV, 75 eV)/C(KLL, 260 eV).

Fig. 33 Changes in N/Si ratio of Si_3N_4 as functions of hydrogen fluence and Ar^+ ion fluence.

Fig. 34 Changes in O/Si ratio of SiO_2 as functions of hydrogen fluence and Ar^+ ion fluence.

Fig. 35 C1s XPS spectra of SiC before and after 6 keV H_2^+-ion bombardments. An arrow indicates position of C1s line for graphite target bombarded with H_2^+ ions, taken from Fig.36.

Fig. 36 C1s XPS spectra of graphite before and after 6keV H_2^+-ion bombardments.

Fig. 37 Si2p XPS spectra of Si_3N_4 before and after 6 keV H_2^+-ion bombardments. An arrow indicates position of Si2p line for Si target bombarded with H_2^+ ions, taken from Fig.39.

Fig. 38 Si2p XPS spectra of SiO_2 before and after 6 keV H_2^+-ion bombardments. An arrow indicates position of Si2p line for Si target bombarded with H_2^+ ions, taken from Fig.39. Hatched area is attributable to silicon hydride(s).

Fig. 39 Si2p XPS spectra of Si before and after 6keV H_2^+-ion bombardments.

Fig. 40 Valence-band XPS spectra before(——) and after(···) 6 keV H_2^+-ion bombardments. Note a peak appeared at around 4 eV of Si target. This is attributable to silicon hydride(s).

1. Introduction

In the latest years, many workers have investigated interactions between refractory materials and energetic hydrogen, in relation with recycling of hydrogen isotopes at first wall in a controlled thermonuclear reactor.[1] Low-Z materials such as carbides, nitrides and borides have been considered as candidate materials of the first wall, because of their less energy-loss through bremsstrahlung in the plasma. Especially, graphite, SiC and TiC are receiving much attention for their good refractoriness. The re-emission behavior of the implanted hydrogen isotopes strongly depends upon their trapped states in the materials. However, there has been only a few works on physical and chemical states of the hydrogen isotopes implanted.[2) By means of X-ray photoelectron spectroscopy(XPS) and X-ray-induced Auger electron spectroscopy(XAES), the present authors have confirmed hydride formation in some of 3d and 4d transition metals bombarded with energetic hydrogen ions.[3-5]

This report presents the intrinsic data of XPS and XAES for graphite, Si, SiC, Si_3N_4 and SiO_2. These materials are characterized by not only their electrical properties as conductor(graphite), semiconductors(Si and SiC) and insulators(Si_3N_4 and SiO_2), but also high strength in mechanical properties as refractory materials(SiC and Si_3N_4). In the later part of this report, the data obtained are applied to quantitative analyses of the changes in the chemical composition of the surface layer caused by bombardments with 6 keV H_2^+ -ions.

2. Experimental

2.1 Materials

Pyrographite from Tokai Carbon Co. Ltd. was introduced into a chamber of an electron spectrometer without any surface treatment except for scraping its surface with a razor blade. Highly pure crystals of Si was obtained from Japan Electronic Metals Co. Ltd. and oxide overlayers on the Si(110) plane was removed by use of a mixed solution of nitric and fluoric acids.

1. Introduction

In the latest years, many workers have investigated interactions between refractory materials and energetic hydrogen, in relation with recycling of hydrogen isotopes at first wall in a controlled thermonuclear reactor.[1] Low-Z materials such as carbides, nitrides and borides have been considered as candidate materials of the first wall, because of their less energy-loss through bremsstrahlung in the plasma. Especially, graphite, SiC and TiC are receiving much attention for their good refractoriness. The re-emission behavior of the implanted hydrogen isotopes strongly depends upon their trapped states in the materials. However, there has been only a few works on physical and chemical states of the hydrogen isotopes implanted.[2] By means of X-ray photoelectron spectroscopy(XPS) and X-ray-induced Auger electron spectroscopy(XAES), the present authors have confirmed hydride formation in some of 3d and 4d transition metals bombarded with energetic hydrogen ions.[3-5]

This report presents the intrinsic data of XPS and XAES for graphite, Si, SiC, Si_3N_4 and SiO_2. These materials are characterized by not only their electrical properties as conductor(graphite), semiconductors(Si and SiC) and insulators(Si_3N_4 and SiO_2), but also high strength in mechanical properties as refractory materials(SiC and Si_3N_4). In the later part of this report, the data obtained are applied to quantitative analyses of the changes in the chemical composition of the surface layer caused by bombardments with 6 keV H_2^+ -ions.

2. Experimental

2.1 Materials

Pyrographite from Tokai Carbon Co. Ltd. was introduced into a chamber of an electron spectrometer without any surface treatment except for scraping its surface with a razor blade. Highly pure crystals of Si was obtained from Japan Electronic Metals Co. Ltd. and oxide overlayers on the Si(110) plane was removed by use of a mixed solution of nitric and fluoric acids.

SiC and Si_3N_4 were of ∿100 μm thickness deposited on graphite substrate by CVD method in Toshiba Ceramics Co. Ltd. SiO_2 was pure quartz of ∿300 μm thickness. These three samples were polished into mirrorlike plane by use of 1/4 micron diamond paste and mounted on sample holders using silver paste.

Sample surfaces were chemically cleaned by heating the holder with the specimen at 350 °C for 3 hours under a pressure of $\sim 10^{-7}$ Pa, and then Ar^+-ion etching was performed at room temperature for the elimination of the carbon and/or oxygen containing adsorbates. A faint beam(ca. 4 $\mu A/cm^2$) of 8 keV Ar^+-ion proved to be effective for this purpose, and it caused no compositional changes in the surface regions of the samples themselves except for SiO_2.

2.2 Spectral measurements

The XPS and XAES measurements were carried out by means of a V.G.ESCALAB-5 spectrometer, as previously described.[3] Briefly, the base pressure during the measurements was less than 1.3×10^{-8} Pa. An Mg Kα X-ray source(1253.6 eV) was operated at 125 W(12.5 kV x 10 mA). The spectrometer was calibrated such that the $4f_{7/2}$ line of metallic gold appears at E_b = 84.0 eV. Because of charging effect during the XPS measurements an original spectrum of Si_3N_4 shifted by ∿5 eV to higher binding-energy side. Therefore, the energy scale was aligned to make the O1s lines(E_b = 532.4 eV) from the adsorbates on Si_3N_4 surface and from those on SiC surface coincide. For the XAES measurements of the Si(KLL) region($E_k \simeq 1615$ eV), accumulation for over 80 minutes was required for good S/N ratio, while 20 minutes accumulation was enough for the determination of the spectral pattern of the core lines.

3. Results and discussion

The XPS and XAES spectra for graphite are presented in Figs.1-4, for Si in Figs.5-10, for SiC in Figs.11-17, for Si_3N_4 in Figs.18-24 and for SiO_2 in Figs.25-31, respectively. In these figures, the peak

SiC and Si_3N_4 were of $\sim$100 μm thickness deposited on graphite substrate by CVD method in Toshiba Ceramics Co. Ltd. SiO_2 was pure quartz of $\sim$300 μm thickness. These three samples were polished into mirrorlike plane by use of 1/4 micron diamond paste and mounted on sample holders using silver paste.

Sample surfaces were chemically cleaned by heating the holder with the specimen at 350 °C for 3 hours under a pressure of $\sim 10^{-7}$ Pa, and then Ar^+-ion etching was performed at room temperature for the elimination of the carbon and/or oxygen containing adsorbates. A faint beam(ca. 4 $\mu A/cm^2$) of 8 keV Ar^+-ion proved to be effective for this purpose, and it caused no compositional changes in the surface regions of the samples themselves except for SiO_2.

2.2 Spectral measurements

The XPS and XAES measurements were carried out by means of a V.G.ESCALAB-5 spectrometer, as previously described.[3] Briefly, the base pressure during the measurements was less than 1.3×10^{-8} Pa. An Mg Kα X-ray source(1253.6 eV) was operated at 125 W(12.5 kV x 10 mA). The spectrometer was calibrated such that the $4f_{7/2}$ line of metallic gold appears at E_b = 84.0 eV. Because of charging effect during the XPS measurements an original spectrum of Si_3N_4 shifted by $\sim$5 eV to higher binding-energy side. Therefore, the energy scale was aligned to make the O1s lines(E_b = 532.4 eV) from the adsorbates on Si_3N_4 surface and from those on SiC surface coincide. For the XAES measurements of the Si(KLL) region($E_k \simeq 1615$ eV), accumulation for over 80 minutes was required for good S/N ratio, while 20 minutes accumulation was enough for the determination of the spectral pattern of the core lines.

3. Results and discussion

The XPS and XAES spectra for graphite are presented in Figs.1-4, for Si in Figs.5-10, for SiC in Figs.11-17, for Si_3N_4 in Figs.18-24 and for SiO_2 in Figs.25-31, respectively. In these figures, the peak

positions are given in eV. The binding energies of the core lines are summarized in Table 1. The values in the parentheses are energies of the C1s and/or O1s lines from the adsorbates on the surface. The kinetic energies of the Auger peaks are listed in Table 2. These data are useful for the two-dimensional chemical-state plot,[6] because the chemical shifts of the Si(KLL) Auger line are greater and thus permit more accurate identification of a chemical state. It is well known that silicon-containing systems provide prominent energy-loss peaks by the excitation of collective oscillations of the valence electrons.[7,8] These are clearly seen for Si in Fig.5, for SiC in Fig.11 and for Si_3N_4 in Fig.18. The loss energies determined for the present materials are 17 - 20 eV, as shown in Table 3. These data are comparable to values reported previously.[7,8] Peak intensity ratios, which provide important information on the chemical composition of the near surface, are summarized in Table 4. The experimental values obtained by the Ar^+ -ion etching are in agreement with theoretical values estimated from the photoionization cross-section by Scofield.[9] The results lead to a conclusion that the ion etching worked well for removing the adsorbates and did not brought about any drastic changes in the chemical composition of near surface of the samples. In the case of bombardment of SiO_2 with 0.5 keV Ar^+-ion, however, Görlish et.al.[10] have found appreciable changes in the Si2s region, accompanied with a decrease in the O/Si ratio. We have also confirmed the gradual decrease in the O1s/Si2p intensity-ratio(6.45 → 6.13) for the prolonged etching of SiO_2. Both of these are considered to be due to chemical damage induced by the radiation.

Figures 32-40 show H_2^+-bombardment effect upon changes in the chemical composition of the near surface. It is well known that the low-energy hydrogen bombardment of SiC creates a silicon depleted layer on near surface.[11,12] The data given in Figs.32, 35 and 36 add important information to the previous observation. First, the compositional change is predominant on top surface, because the change in the C/Si ratio determined by XPS is less than that by AES whose resolution of the escape depth(∿4 A) is superior to that of XPS(∿15

A). Thus the silicon depleted layer is easily removed by the Ar^+-ion etching, as shown in Fig.32. Since the etching rate is ca. 50 A per a fluence of 1 x 10^{17} ions/cm^2, the thickness of the depleted layer is considered to be less than 15 A. Secondly, H_2^+-ion bombardment causes a change in the C1s line, as shown in Fig.35. The shift to the higher binding-energy implies a C-H bond formation, because the C1s line of polymerized carbon locates at ∿285 eV in binding energy. On the other hand, hydrogen bombardments of Si_3N_4 and SiO_2 make their top surfaces silicon abundant, as shown in Figs.33 and 34. The compositional change amounts to 25 % for Si_3N_4 exposed to a fluence of ∿3 x 10^{18} ions/cm^2. The formations of the Si-rich layer seem to be correlated with chemical reactions occurring near surfaces of the target materials. During the bombardments, chemical species including N-H bond and O-H bond would be preferentially sputtered as ions and neutrals from Si_3N_4 and SiO_2 surfaces, respectively. As a result, a formation of Si-H bond would be expected on the target surfaces. These are confirmed from the XPS spectra shown in Fig.38. Formation of reduced chemical species is clearly seen in Fig.38 for SiO_2 bombarded with 6 keV H_2^+-ions. Since photopeaks around 4 eV for both of Si_3N_4 and SiO_2 targets become slightly intense as shown in Fig.40, the reduced species are likely silicon hydride(s). Considering that the 4 eV peak is somewhat larger than the reported energy for Si-H bond(3.3 eV)[13], the hydrogen ions implanted may be trapped at dangling bond sites. Because the compositional changes in near surfaces of multiple component materials caused by the hydrogen-ion bombardment are closely related with sputtering on top surface, it is urgently needed for the elucidation of their mechanisms to observe, in particular, chemically emitted particles including neutral atoms and molecular clusters.

REFERENCES

1) J.Roth, Chemical Sputtering, in: Sputtering by Particle Bombardment II, Ed. by R.Behrisch(Springer-Verlag, Berlin, 1983).
2) S.Nagata, S.Yamaguchi, Y.Fujino, M.Hirabayashi and K.Kamada, J.Nucl. Mater., 128 & 129, 760(1984).
3) Y.Baba and T.A.Sasaki, Surf.Interface Anal., 6, 171(1984).
4) T.A.Sasaki and Y.Baba, Phys.Rev., B31,791(1985).
5) Y.Baba and T.A.Sasaki, in press , J.Nucl.Mater., (1985).
6) C.D.Wagner, D.E.Passoja, H.F.Hillery, T.G.Kinisky, H.A.Six, W.T.Jansen and J.A.Tayler, J.Vac.Sci.Technol., 21, 933(1982).
7) C.H.Chen, J.Silcox and R.Vincent, Phys.Rev., B12, 64(1975).
8) N.P.Bazhanova, V.V.Korablev and N.I.Kochetov, Sov.Phys.Solid State, 24, 1052(1982).
9) J.H.Scofield, J.Electron Spectrosc.Relat.Phenom., 8, 129(1976).
10) E.Görlish, J.Habel, A.Stoch and J.Stoch, J.Solid State Chem., 33, 121(1980).
11) M.Mohri, K.Watanabe and T.Yamashina, J.Nucl.Mater., 75, 7(1978).
12) S.Fukuda, M.Mohri and T.Yamashina, 9th International Vacuum Congress and 5th International Conference on Solid Surfaces(Madrid, 1983) p 192.
13) P.J.Durrant and B.Durrant, Introduction to Advanced Inorganic Chemistry(Williams Clowes and Sons, London, 1970).

Table 1 Binding energies and chemical shifts of core lines. The values in parentheses are determined by accumulating signals from adsorbates for long period of time.

Material	Orbital	E_b(eV)	Chemical shift(eV)	Fig. No.
Graphite	C2s	?		3
	C1s	284.45		2
	(O1s)	(532.8)		
Si	Si3d	3.0		8
	Si3p	9.3		8
	Si3s	22.6		8
	Si2p	99.5		6
	Si2s	150.9		7
	(C1s)	(284.9)		
	(O1s)	(532.1)		
SiC	Si3p	9.9		15
	Si3s	23.0		15
	Si2p	100.4	0.9	12
	Si2s	151.8	0.9	13
	C2s	14		15
	C1s	283.4	-1.1	14
	(O1s)	(532.4)		
Si_3N_4	Si3p	9.9		22
	Si3s	23		22
	Si2p	101.6	2.1	19
	Si2s	152.9	2.0	20
	N2s	19		22
	N1s	397.7		21
	(C1s)	(284.9)		
	(O1s)	(532.4)		

Table 1 (continued).

Material	Orbital	E_b(eV)	Chemical shift(eV)	Fig. No.
SiO_2	Si3s	25		29
	Si2p	103.5	4.0	26
	Si2s	154.6	3.7	27
	O2s	25		29
	O1s	532.8		28
	(C1s)	(284.9)		

Table 2 Kinetic energies and chemical shifts of the Si(LVV) and Si(KLL) XAES lines.

Material	Line	E_k(eV)	Chemical shift(eV)	Fig. No.
Si	Si(LVV)	91.5		9
	Si(KLL)	1616.8		10
SiC	Si(LVV)	90.5	1	16
	Si(KLL)	1615.5	1.3	17
Si_3N_4	Si(LVV)	83	9	23
	Si(KLL)	1612.6	4.2	24
SiO_2	Si(LVV)	no peak		30
	Si(KLL)	1608.4	8.4	31

Table 3 Loss energies of core-line photoelectrons.

Material	Orbital	Loss energy(eV)
Si	Si2p	17.5
	Si2s	17.6
SiC	Si2p	20
	Si2s	20
Si_3N_4	Si2p	19
	Si2s	19
SiO_2	Si2p	17
	Si2s	no peak

Table 4 Peak intensity ratios of C1s/Si2s for SiC, N1s/Si2s for Si_3N_4 and O1s/Si2s for SiO_2. Calculated values are estimated by use of Scofield's cross-section.[9]

Materials	Exp.1	Exp.2	Calc.
SiC	1.11	1.11	1.17
Si_3N_4	2.06	2.05	2.76
SiO_2	6.45	6.13	6.67

Exp.1 and Exp.2 are data for short-time(less than 1 min) and long-time(ca. 30 min) etchings, respectively.

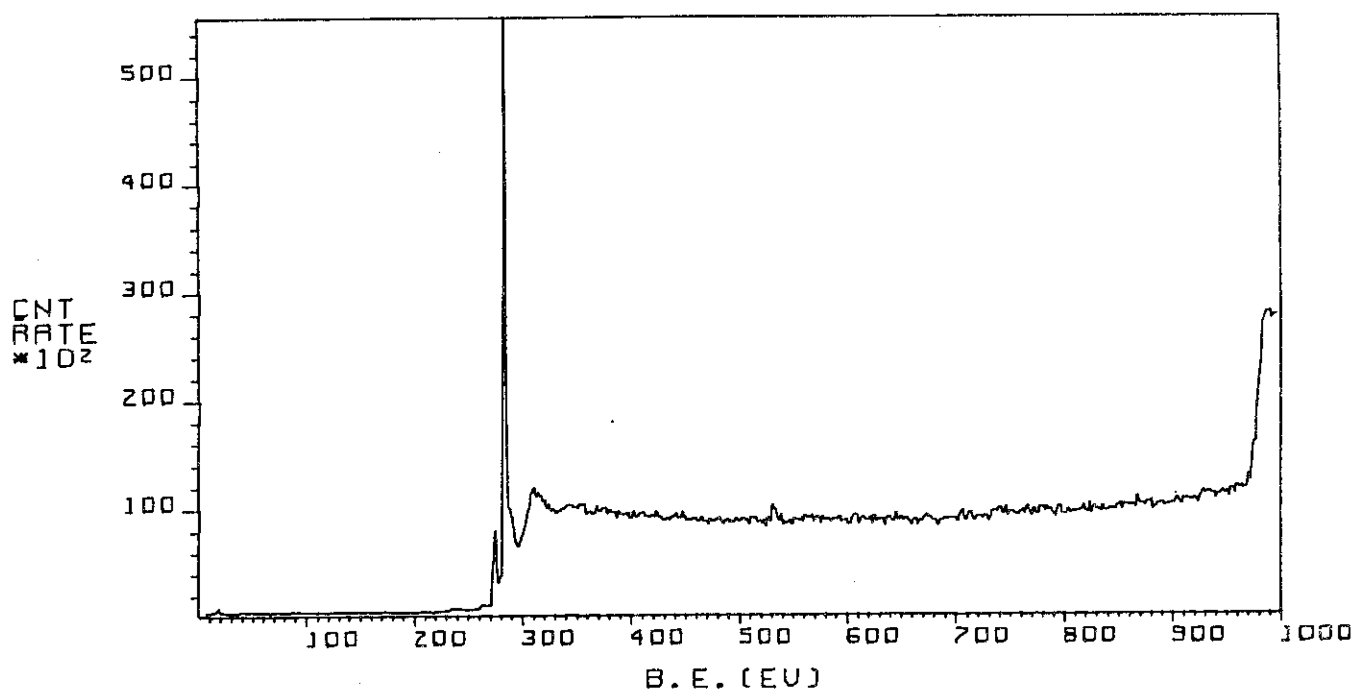

Fig. 1 XPS wide scan of graphite.

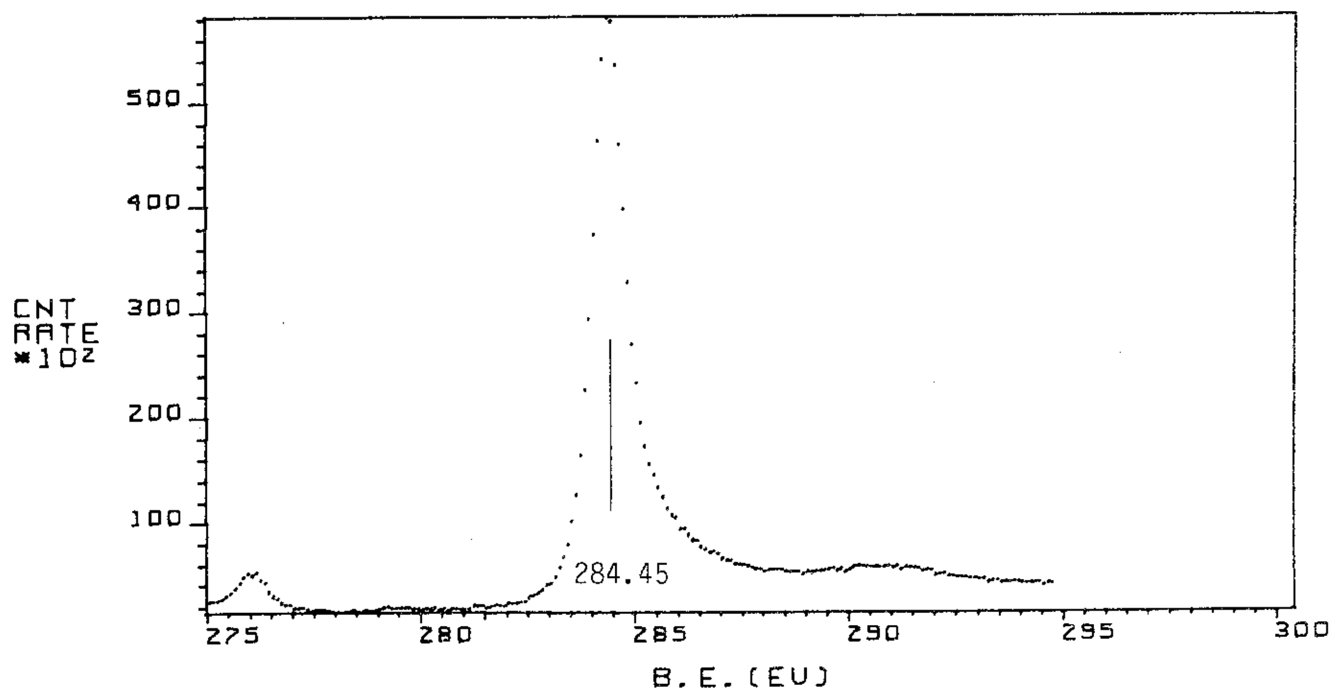

Fig. 2 C1s XPS spectrum of graphite.

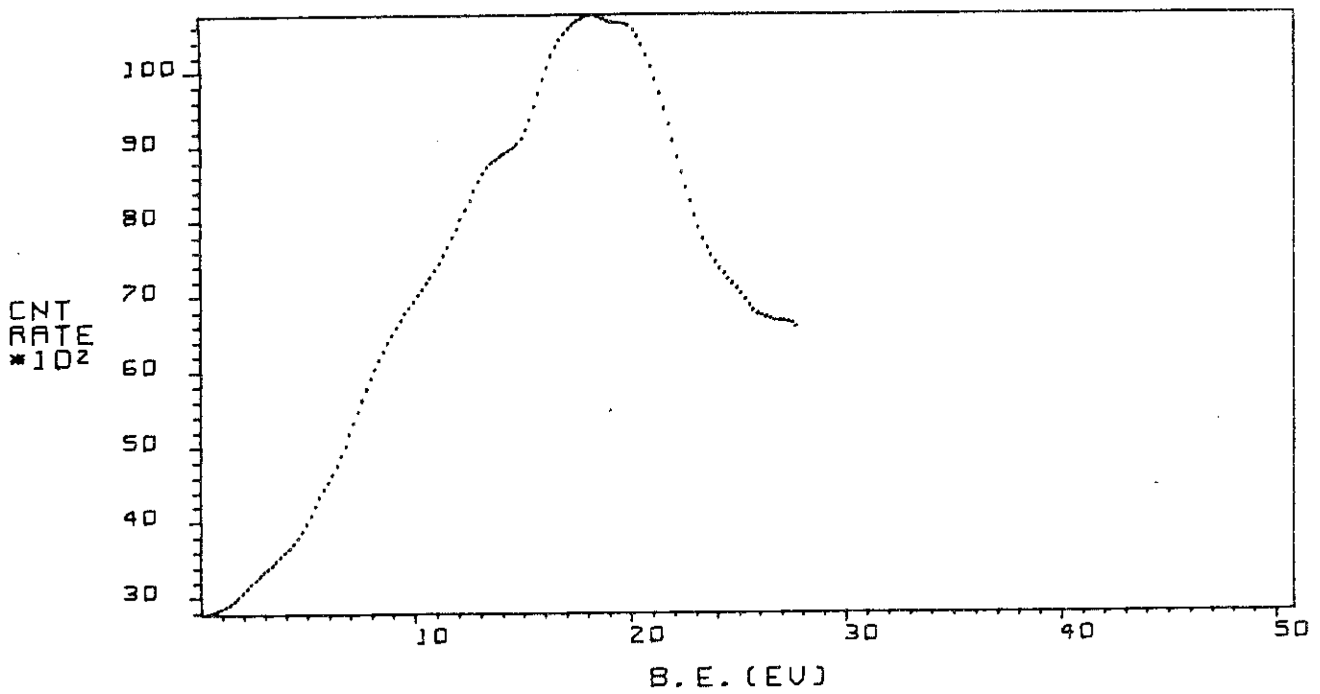

Fig. 3 Valence-band XPS spectrum of graphite.

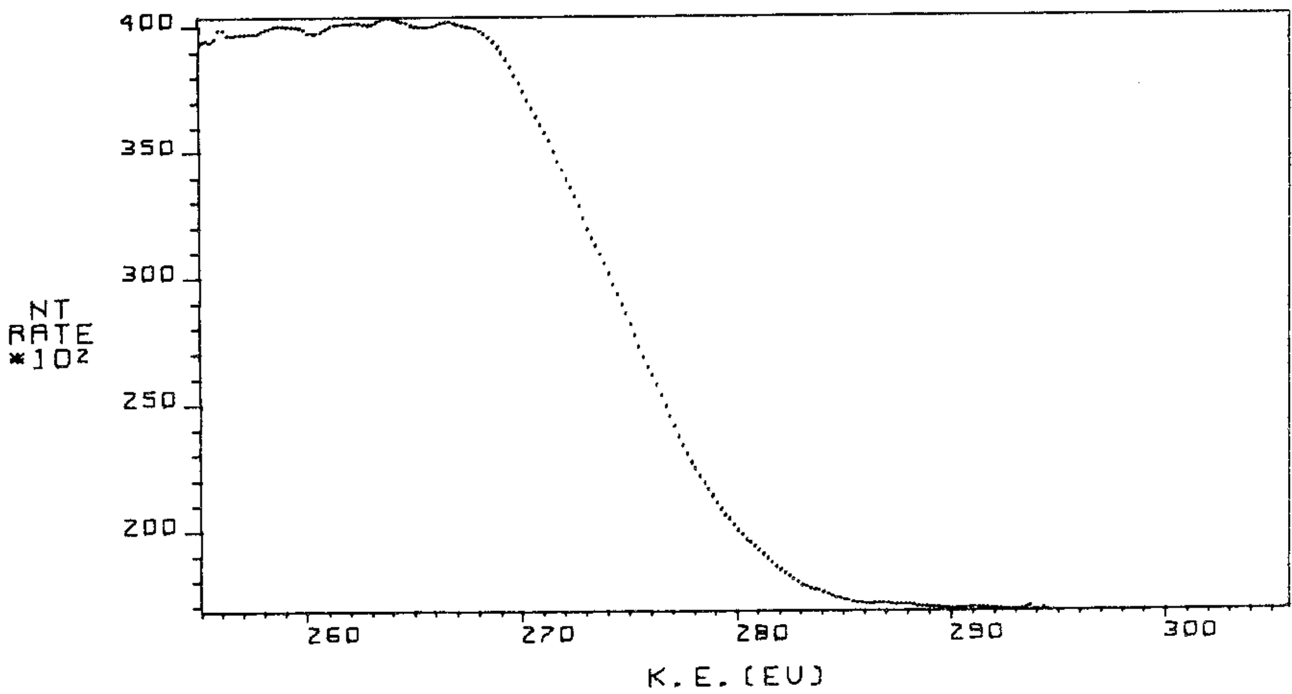

Fig. 4 C(KLL) XAES spectrum of graphite.

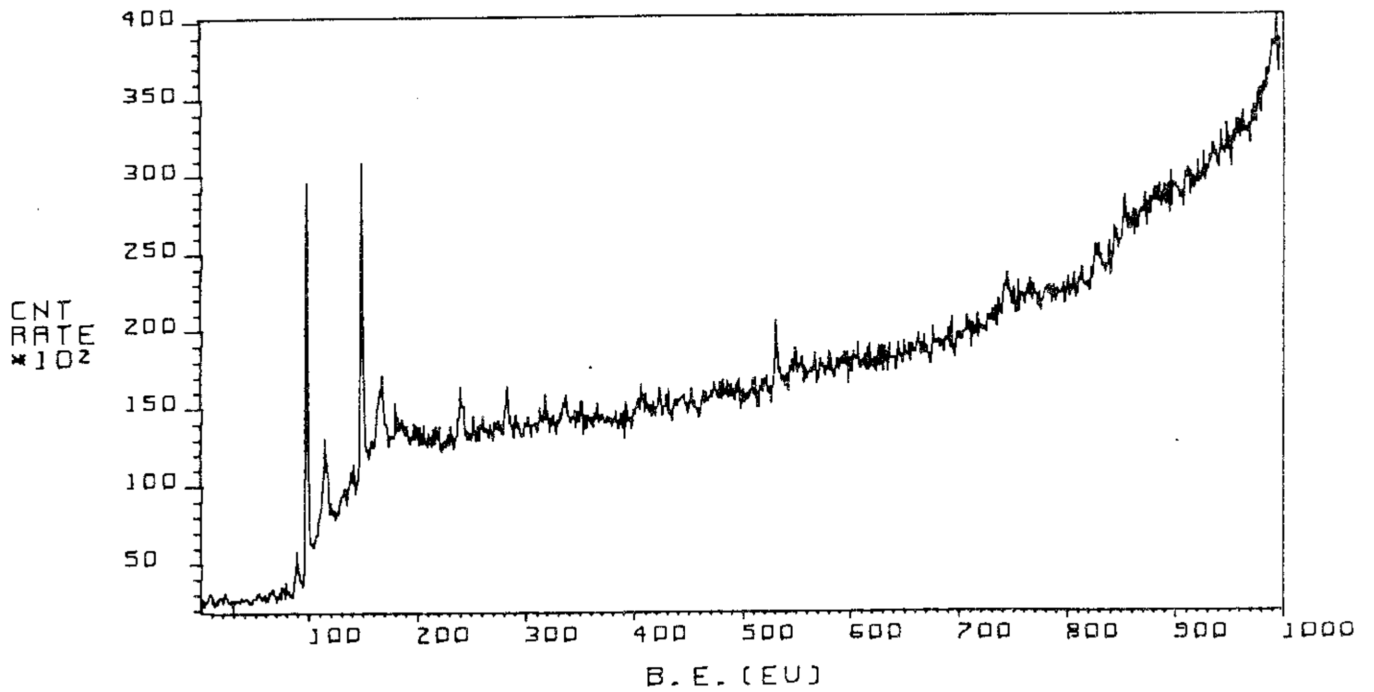

Fig. 5 XPS wide scan of Si.

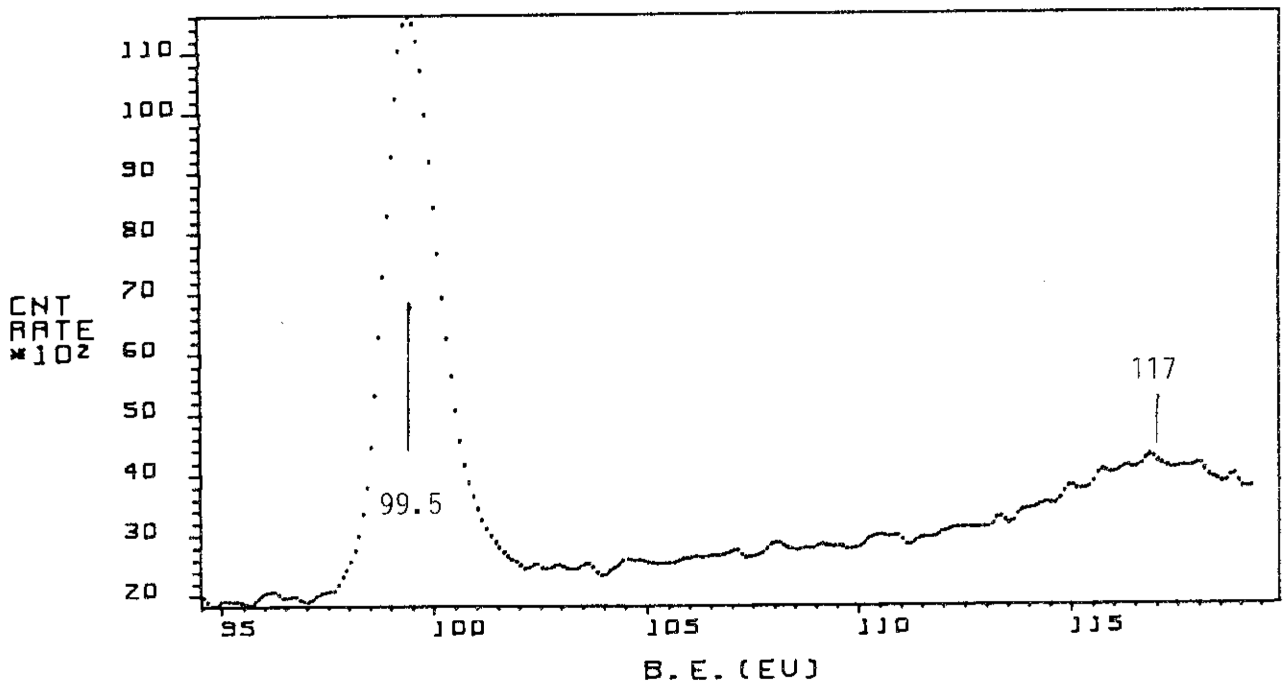

Fig. 6 Si2p XPS spectrum of Si.

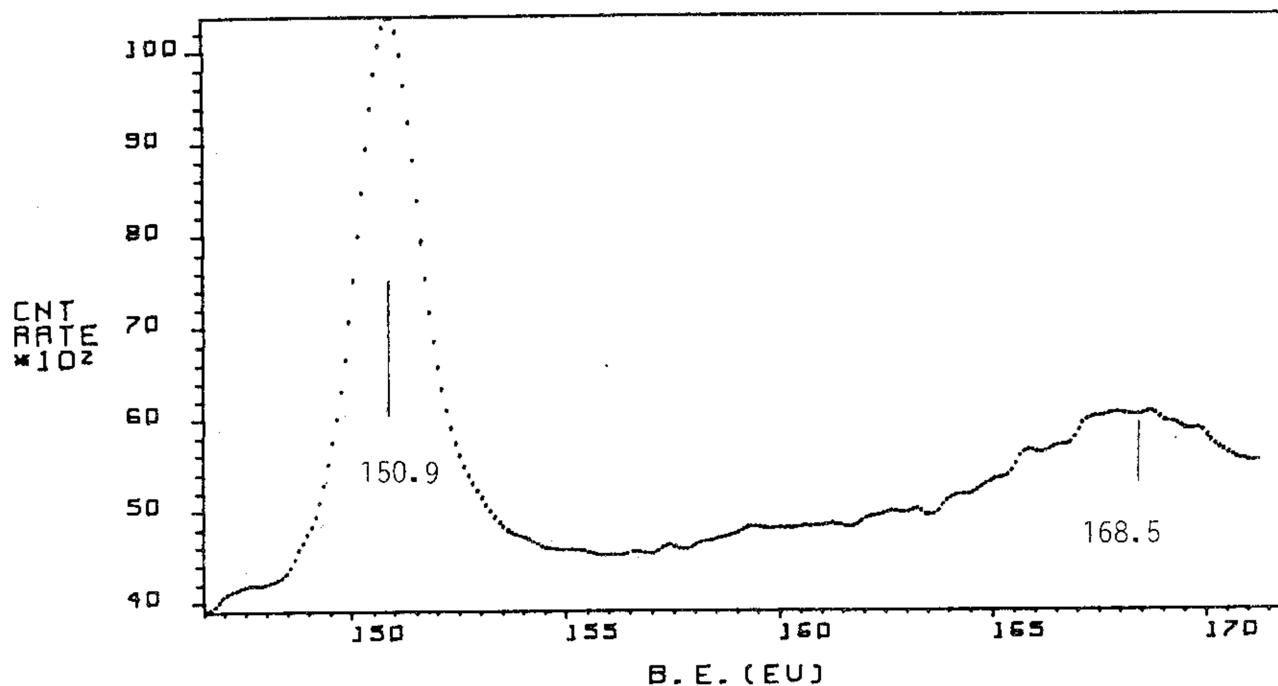

Fig. 7 Si2s XPS spectrum of Si.

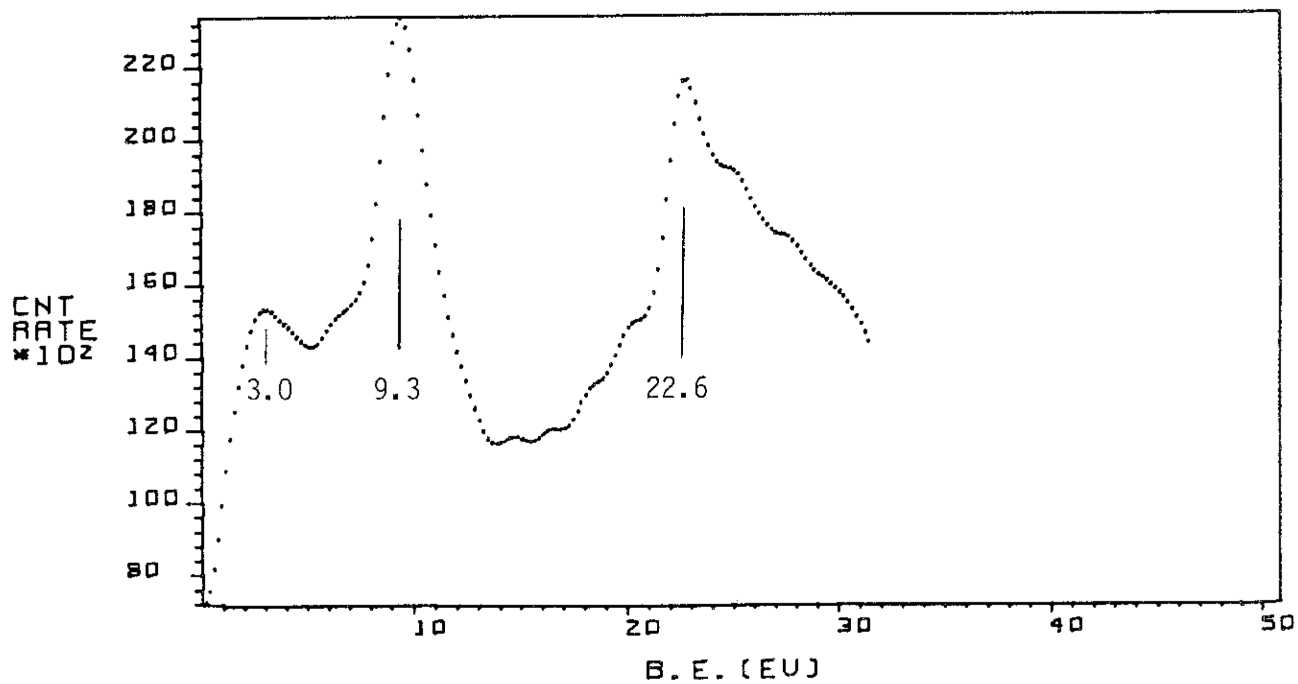

Fig. 8 Valence-band XPS spectrum of Si.

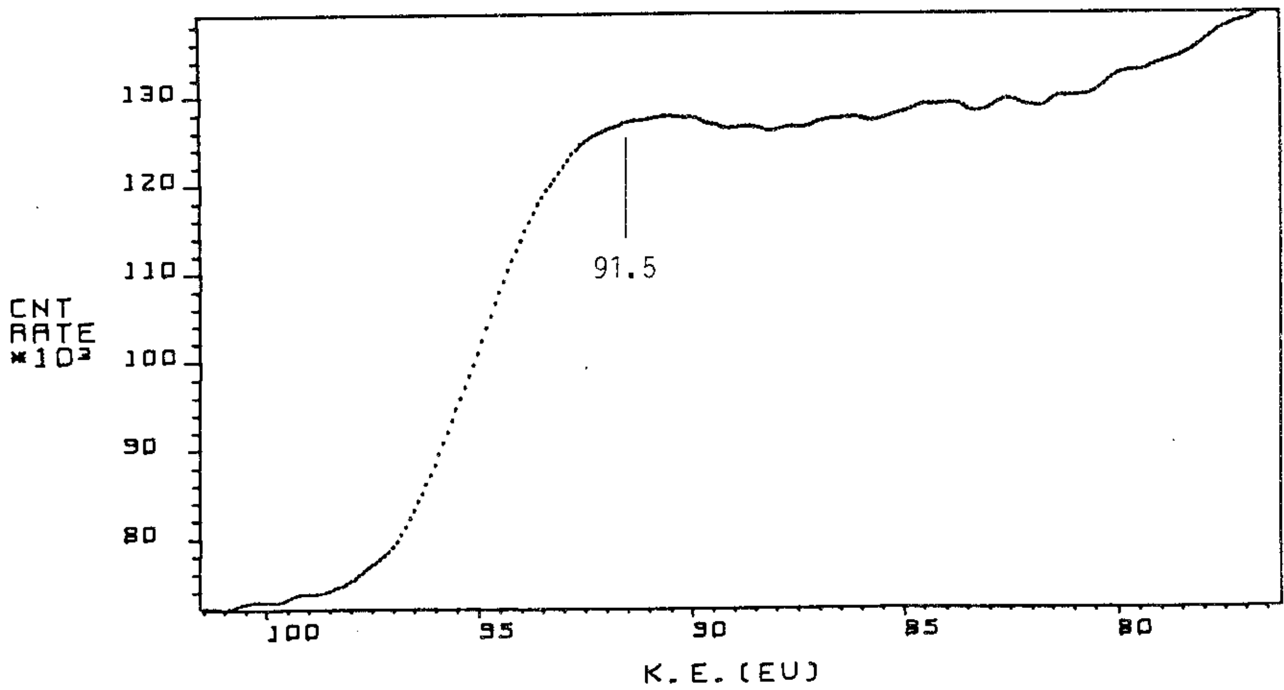

Fig. 9 Si(LVV) XAES spectrum of Si.

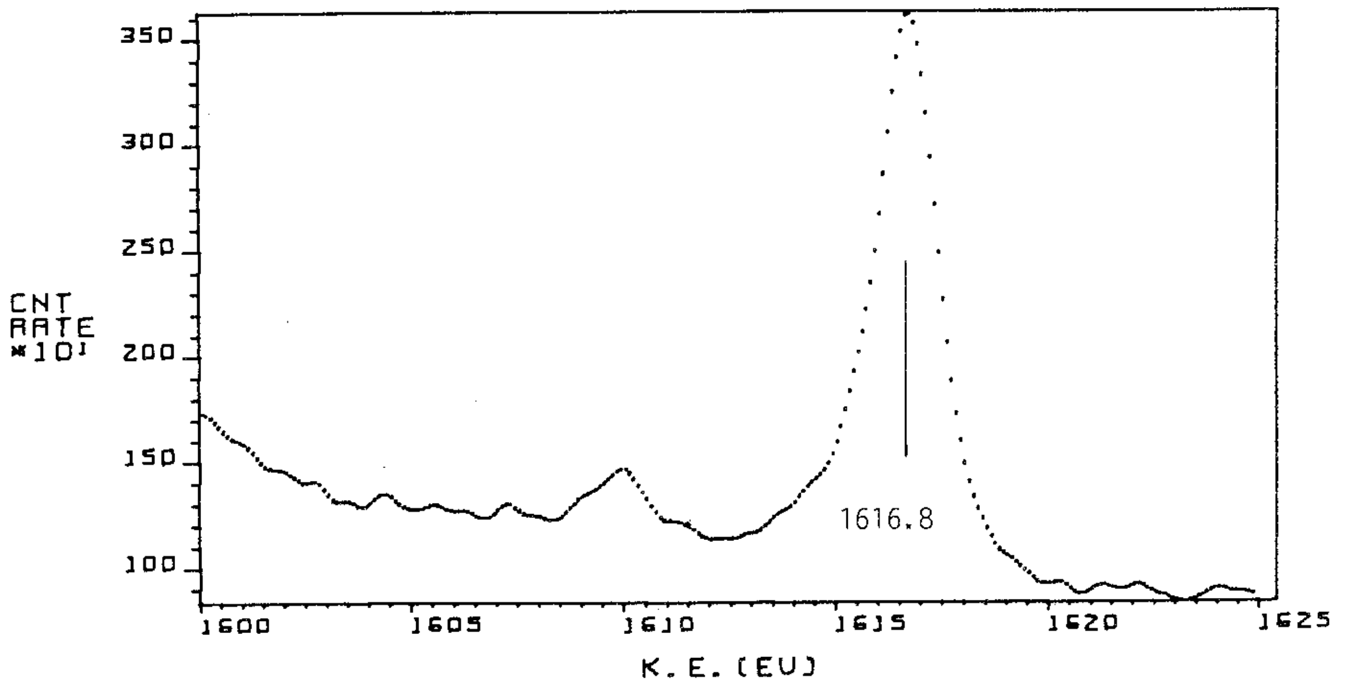

Fig. 10 Si(KLL) XAES spectrum of Si.

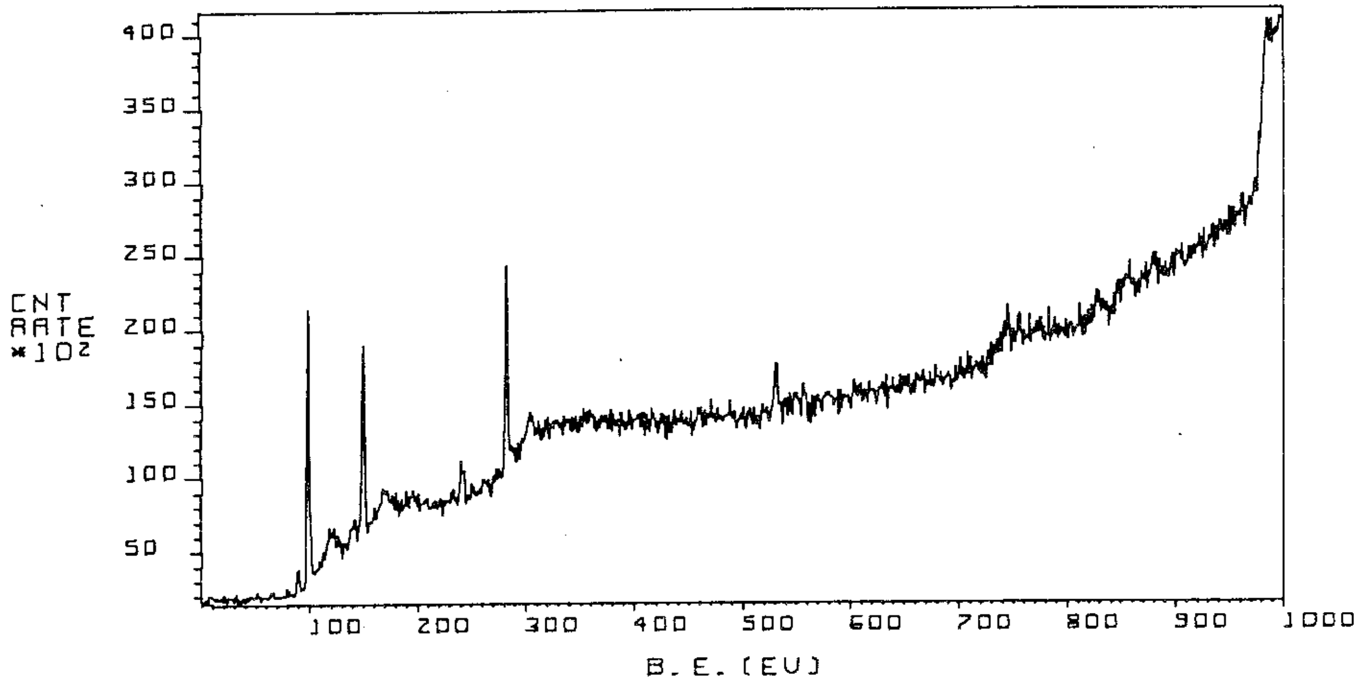

Fig. 11 XPS wide scan of SiC.

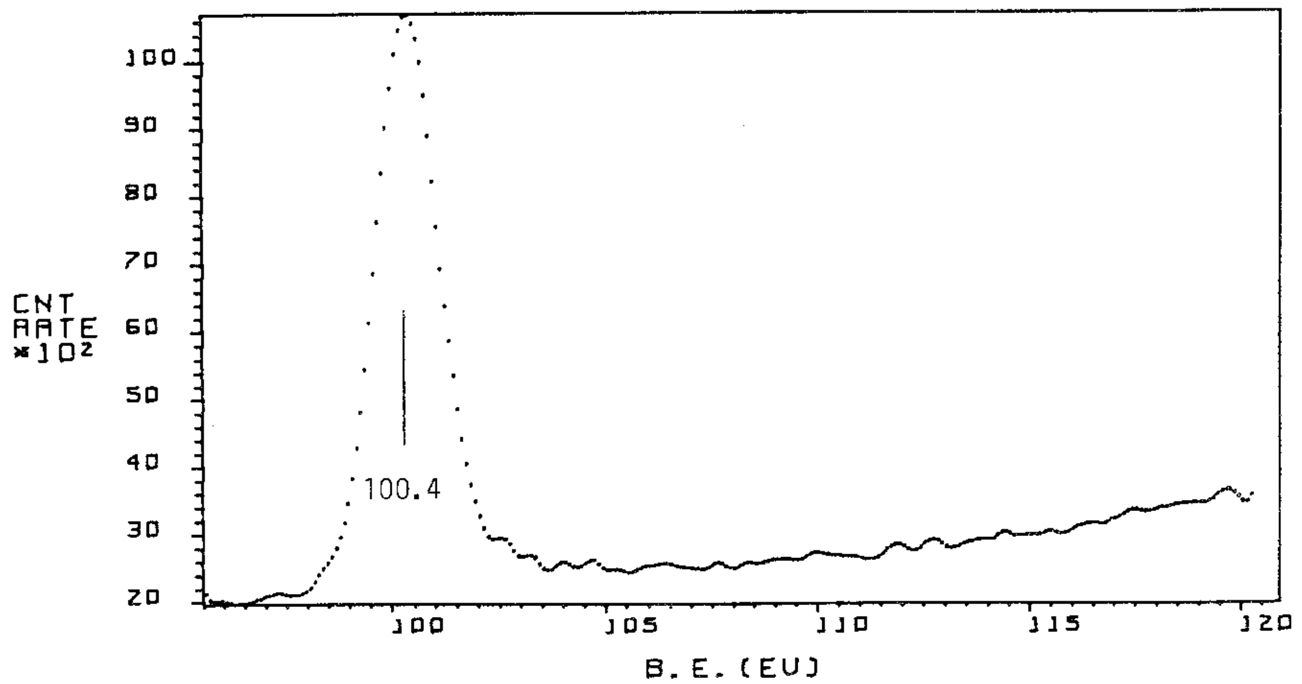

Fig. 12 Si2p XPS spectrum of SiC.

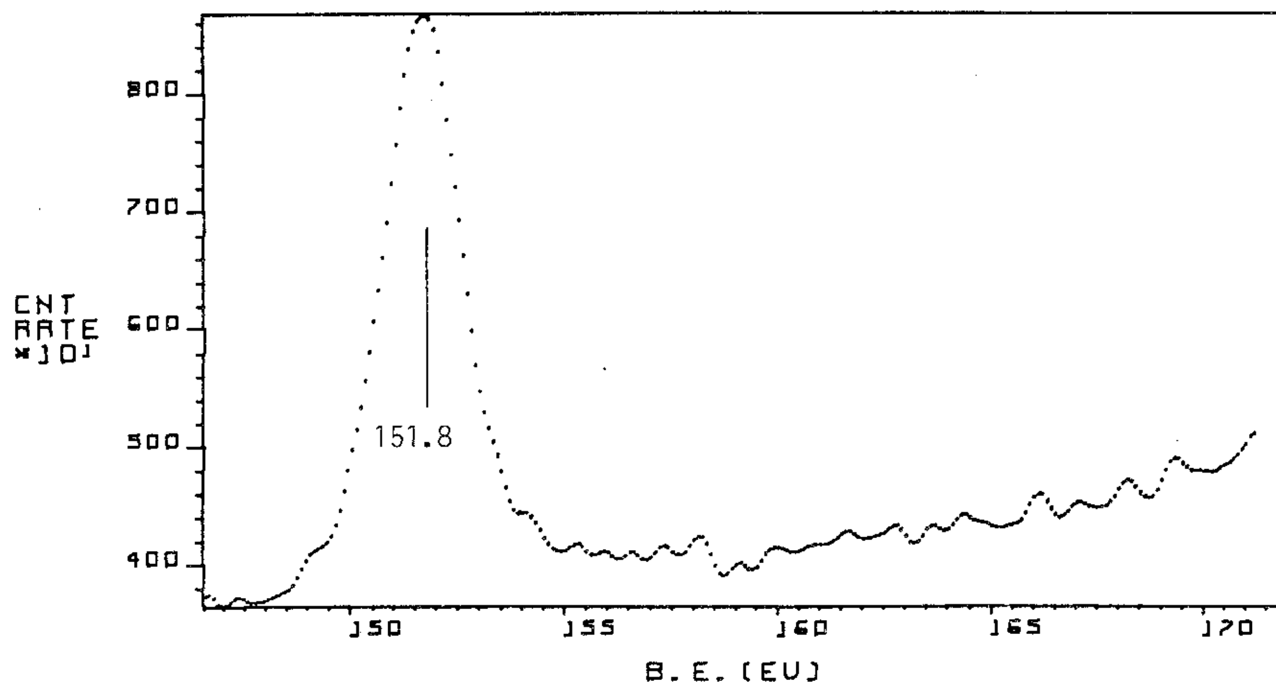

Fig. 13 Si2s XPS spectrum of SiC.

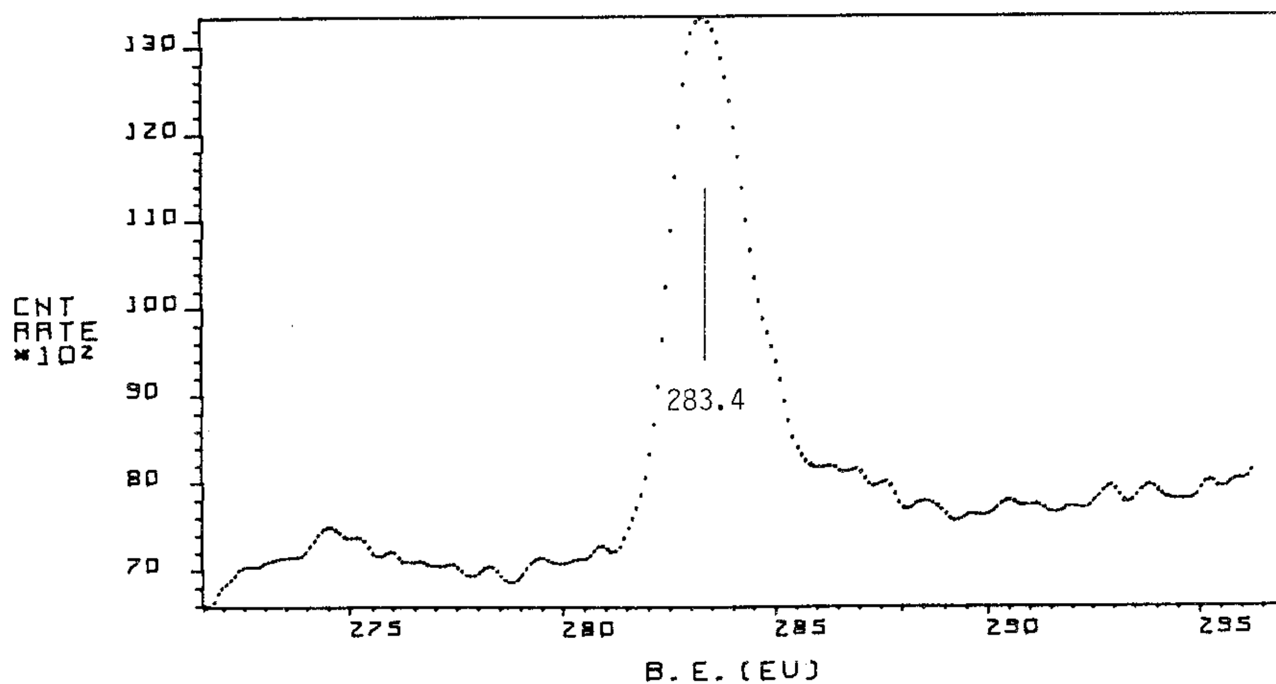

Fig. 14 C1s XPS spectrum of SiC.

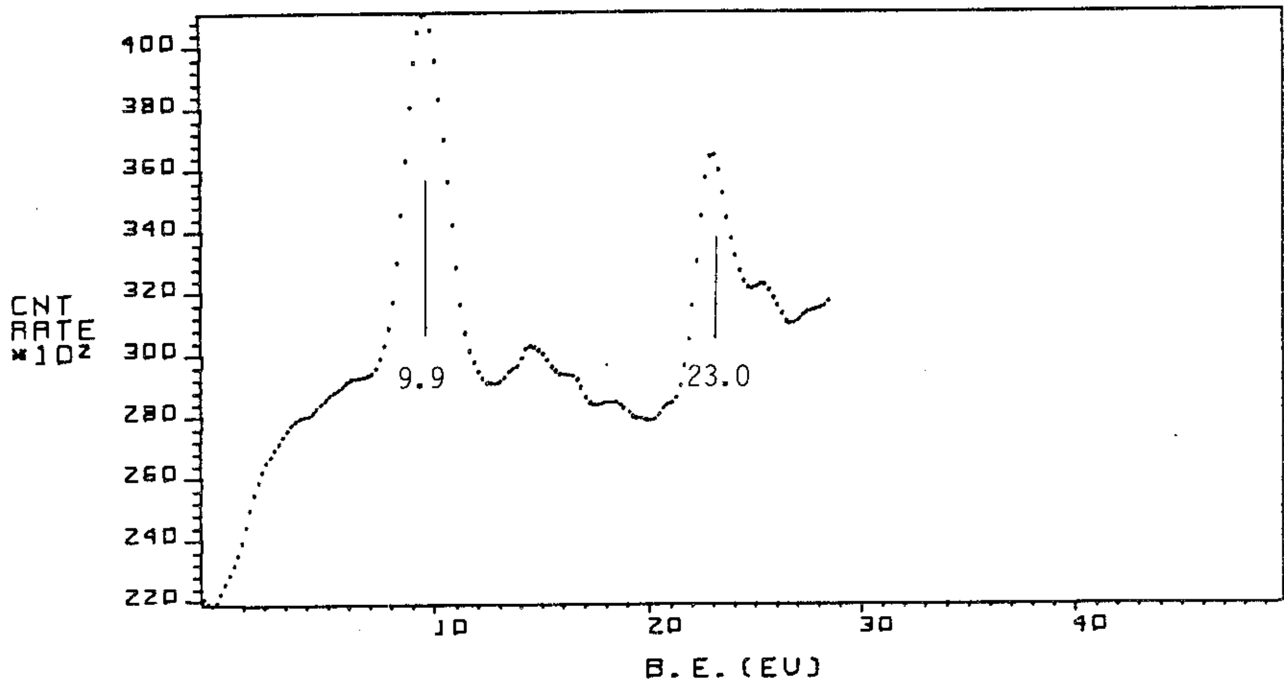

Fig. 15 Valence-band XPS spectrum of SiC.

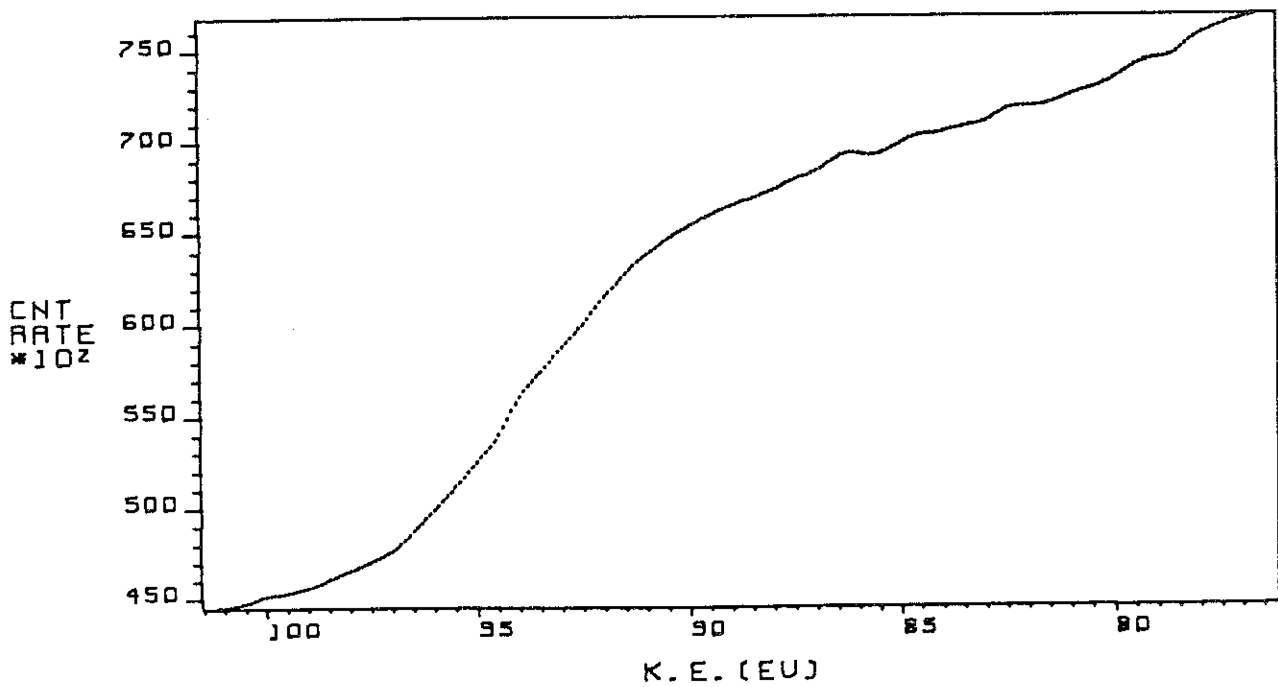

Fig. 16 Si(LVV) XAES spectrum of SiC.

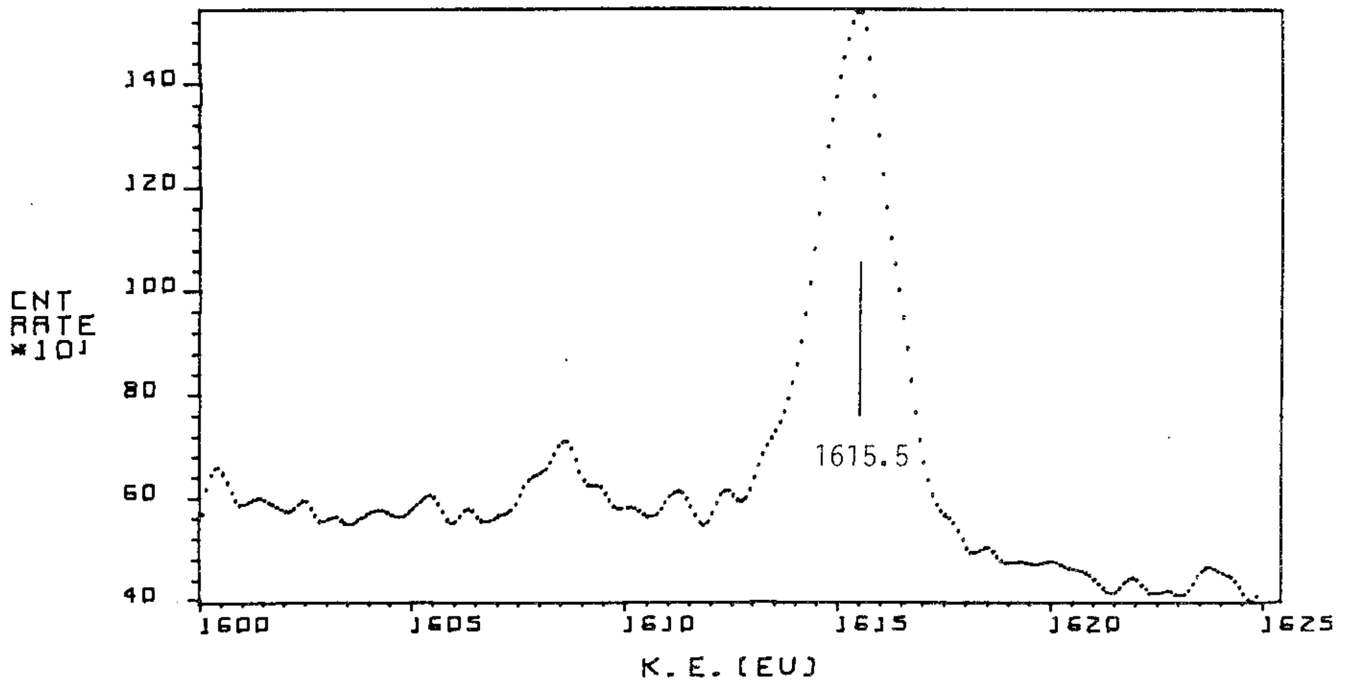

Fig. 17 Si(KLL) XAES spectrum of SiC.

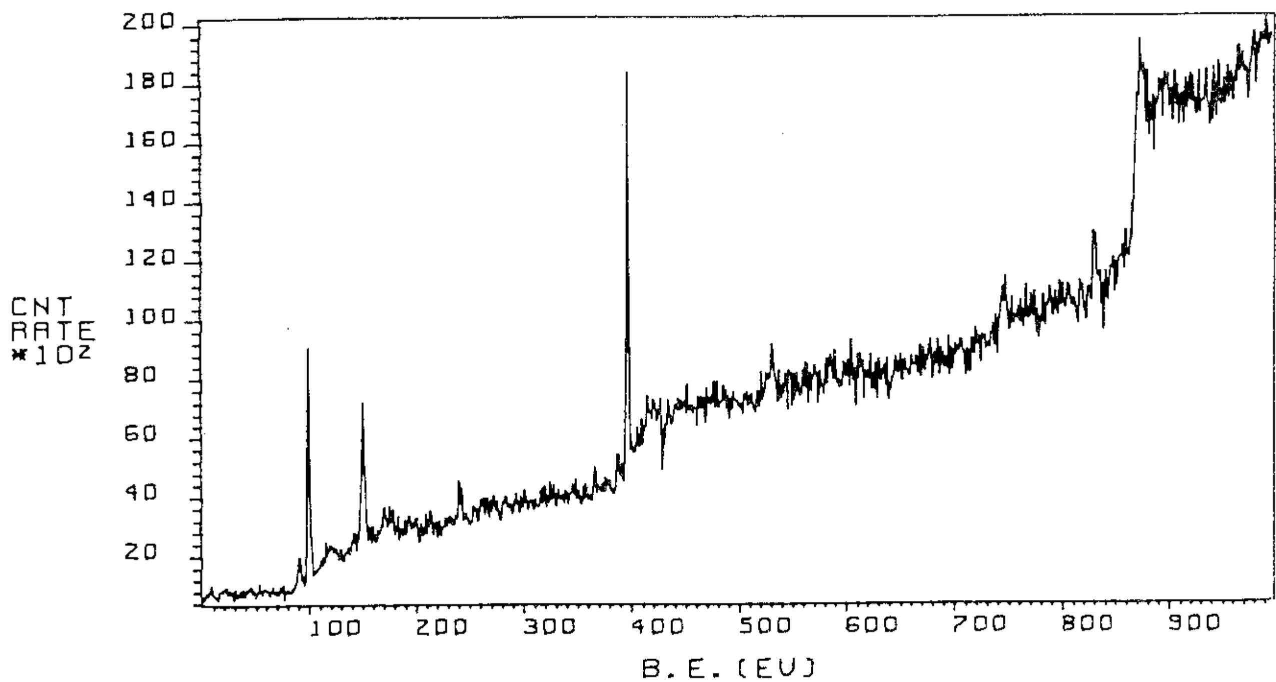

Fig. 18 XPS wide scan of Si_3N_4.

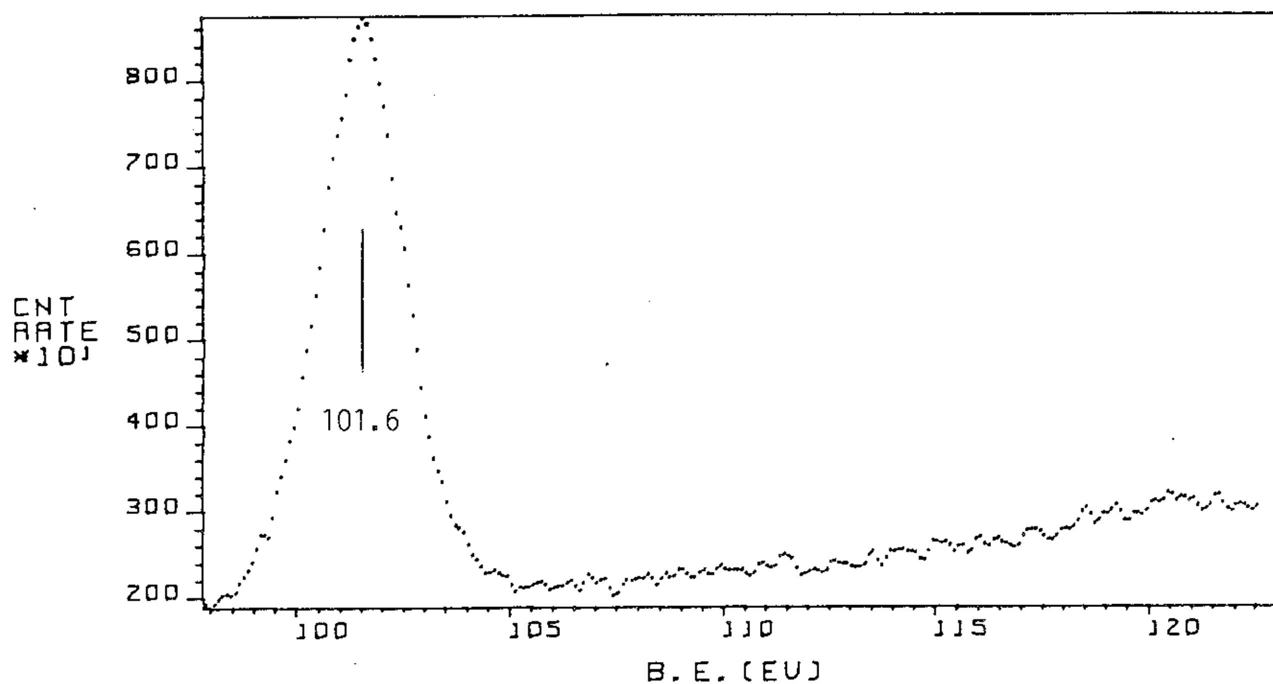

Fig. 19 Si2p XPS spectrum of Si_3N_4.

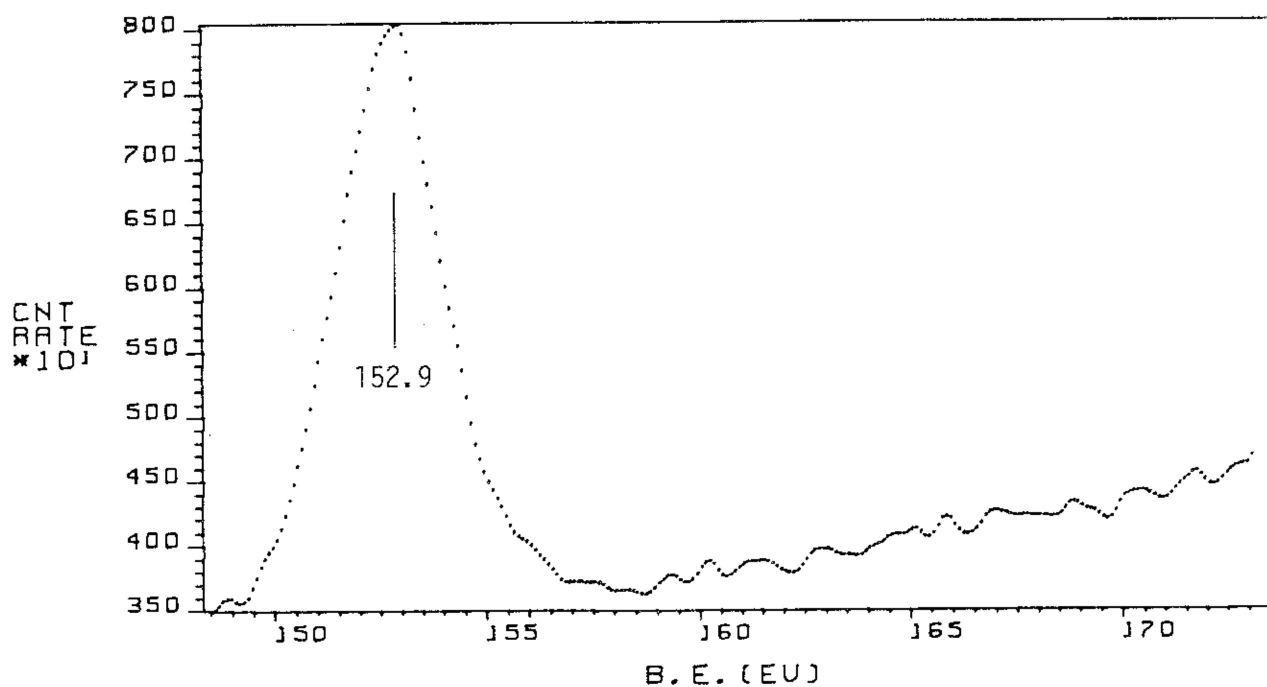

Fig. 20 Si2s XPS spectrum of Si_3N_4.

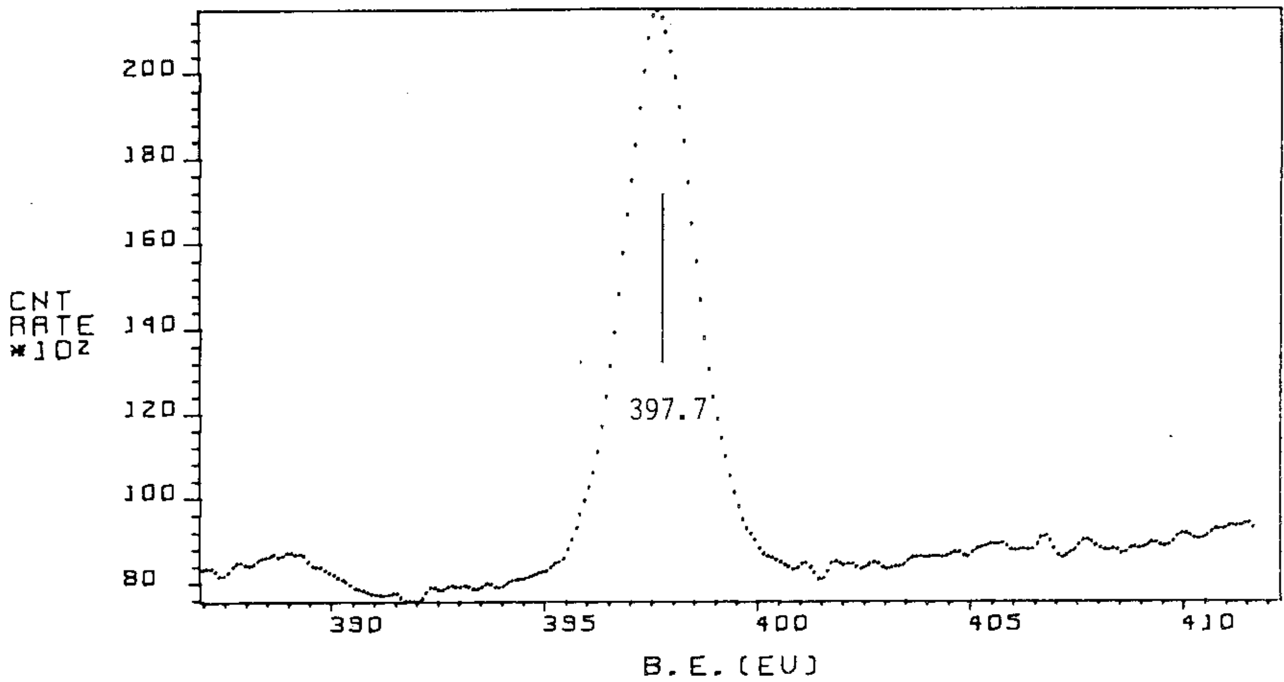

Fig. 21 N1s XPS spectrum of Si_3N_4.

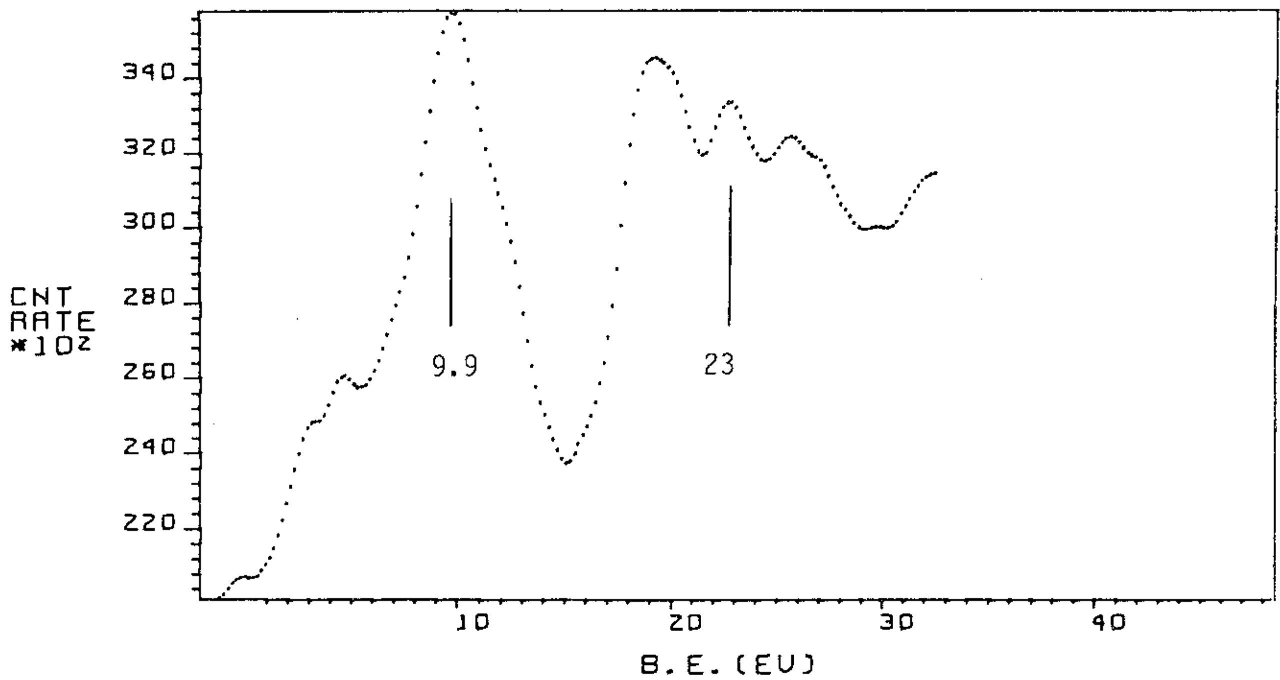

Fig. 22 Valence-band XPS spectrum of Si_3N_4.

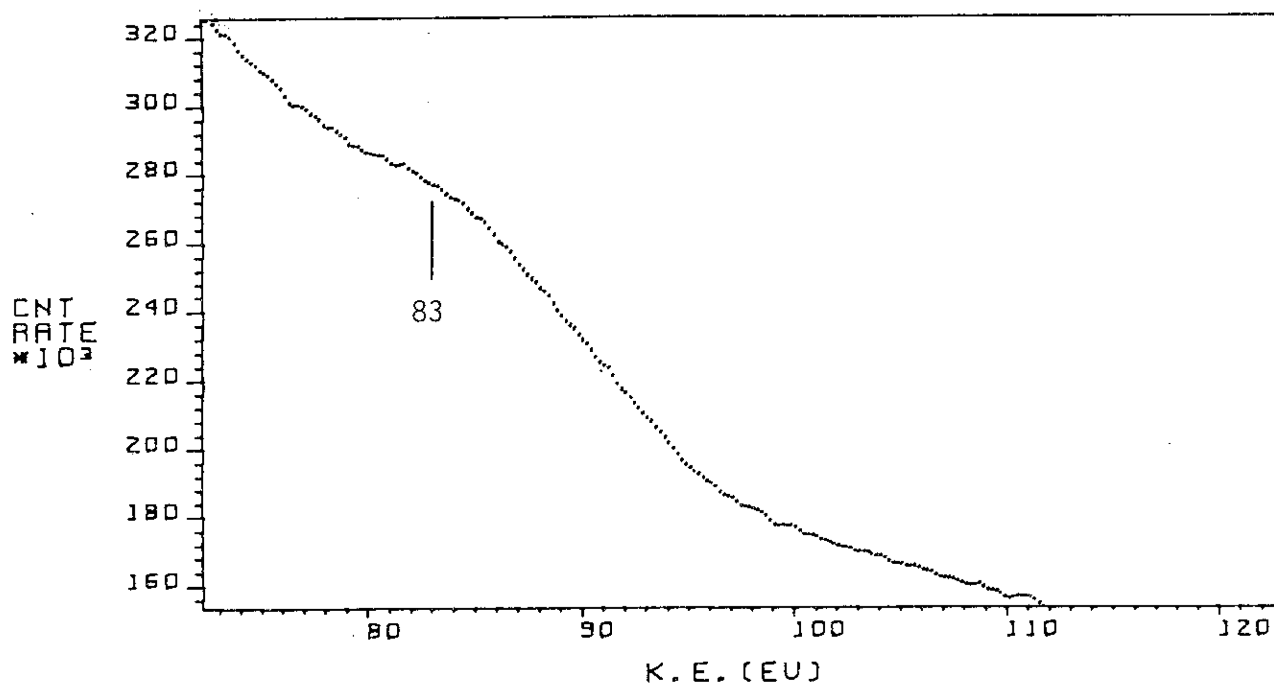

Fig. 23 Si(LVV) XAES spectrum of Si_3N_4.

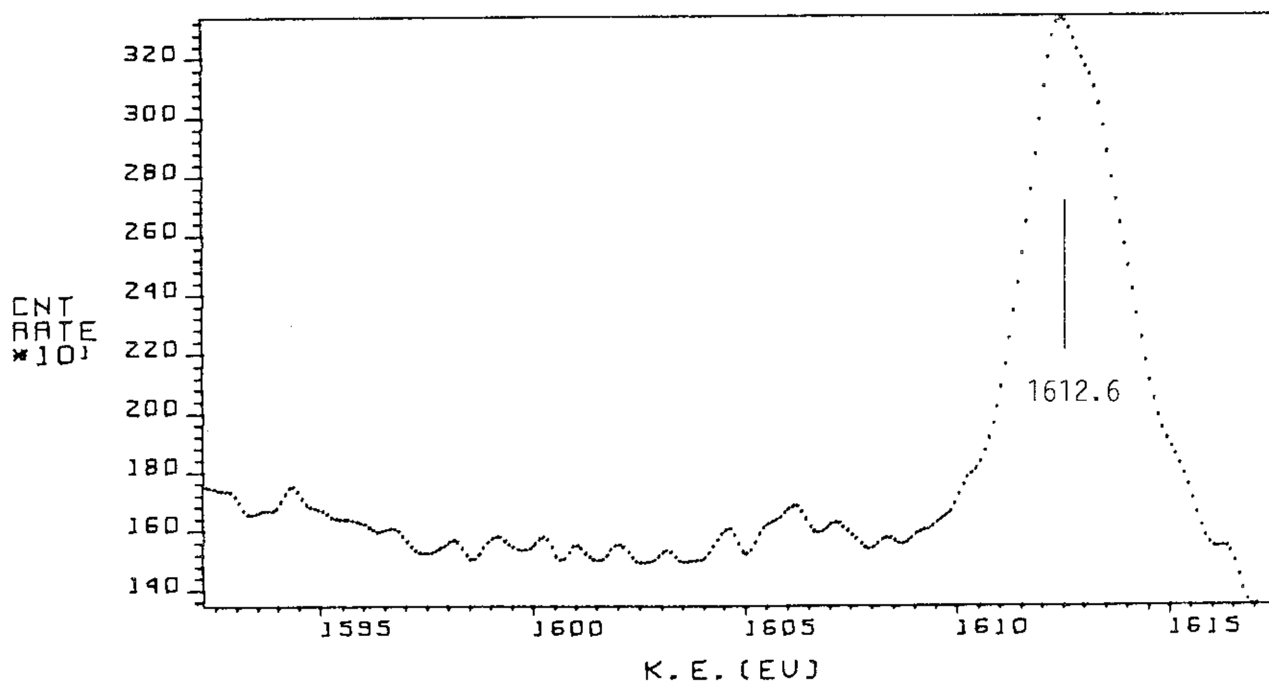

Fig. 24 Si(KLL) XAES spectrum of Si_3N_4.

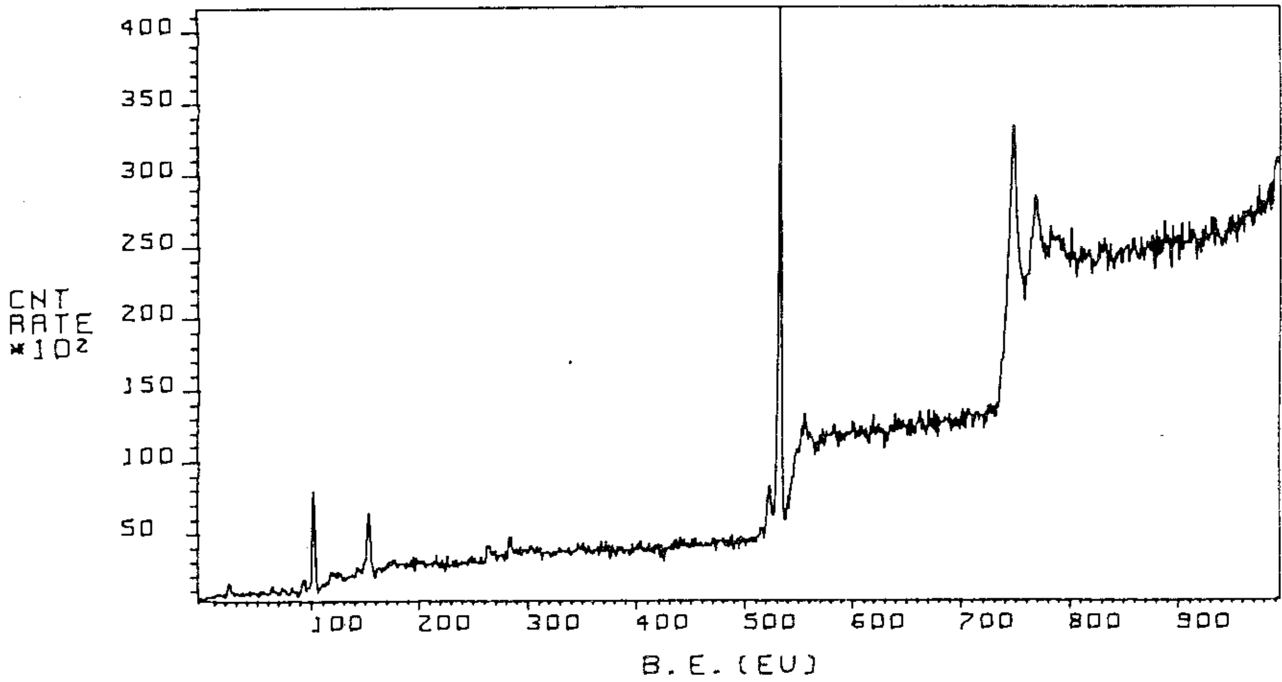

Fig. 25 XPS wide scan of SiO_2.

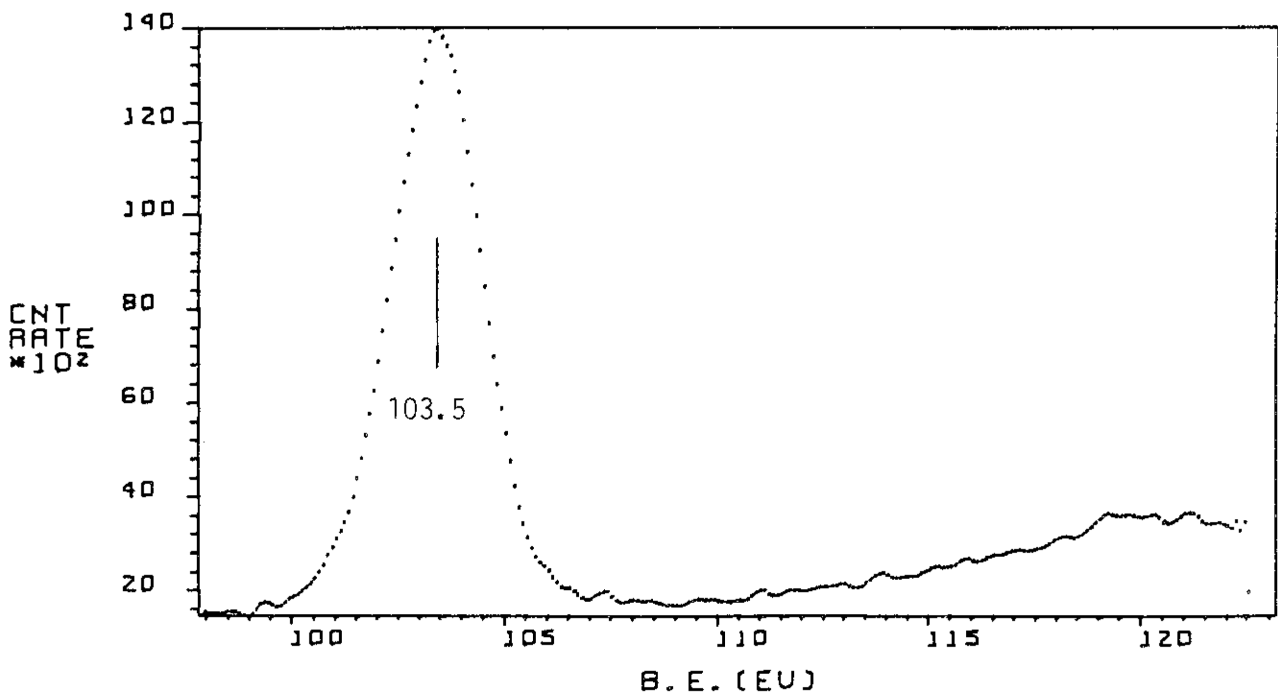

Fig. 26 Si2p XPS spectrum of SiO_2.

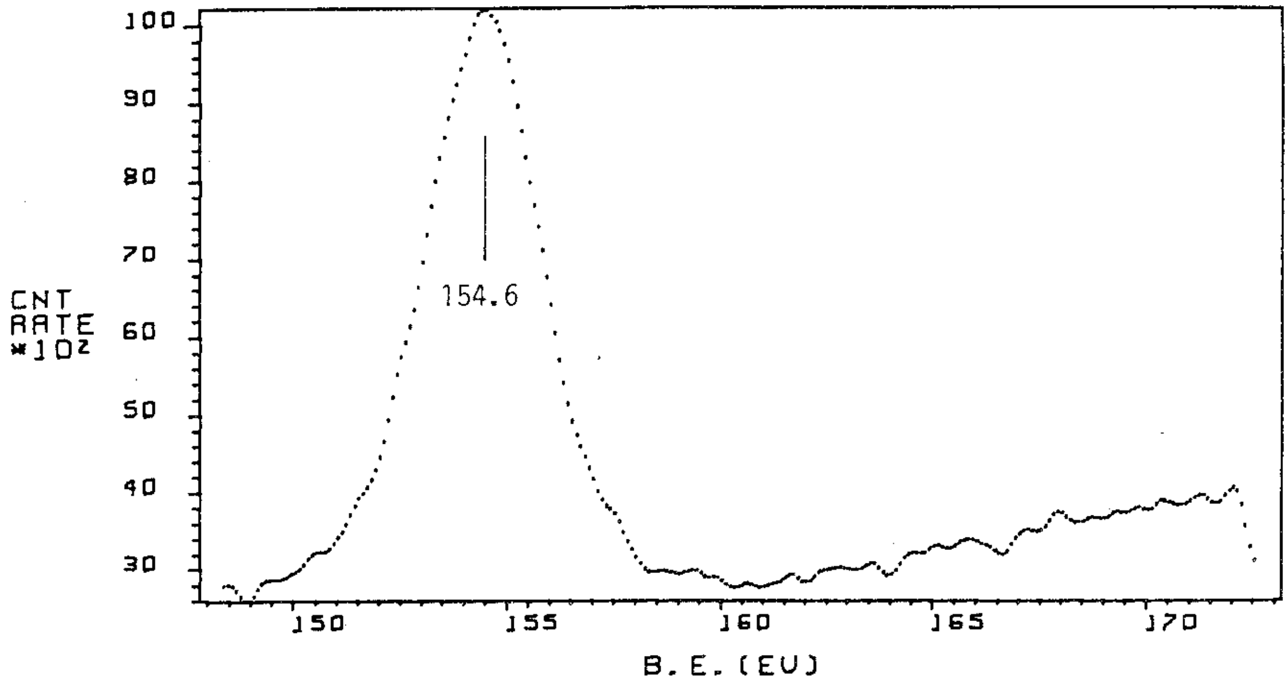

Fig. 27 Si2s XPS spectrum of SiO_2.

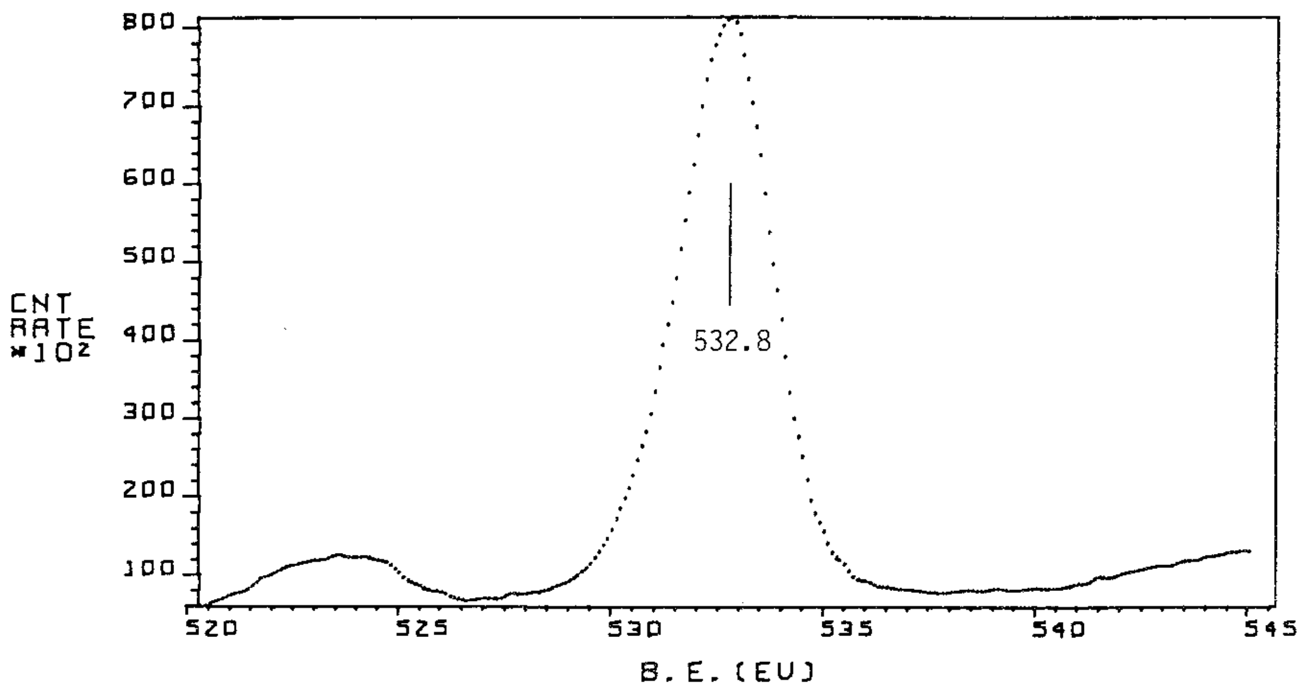

Fig. 28 O1s XPS spectrum of SiO_2.

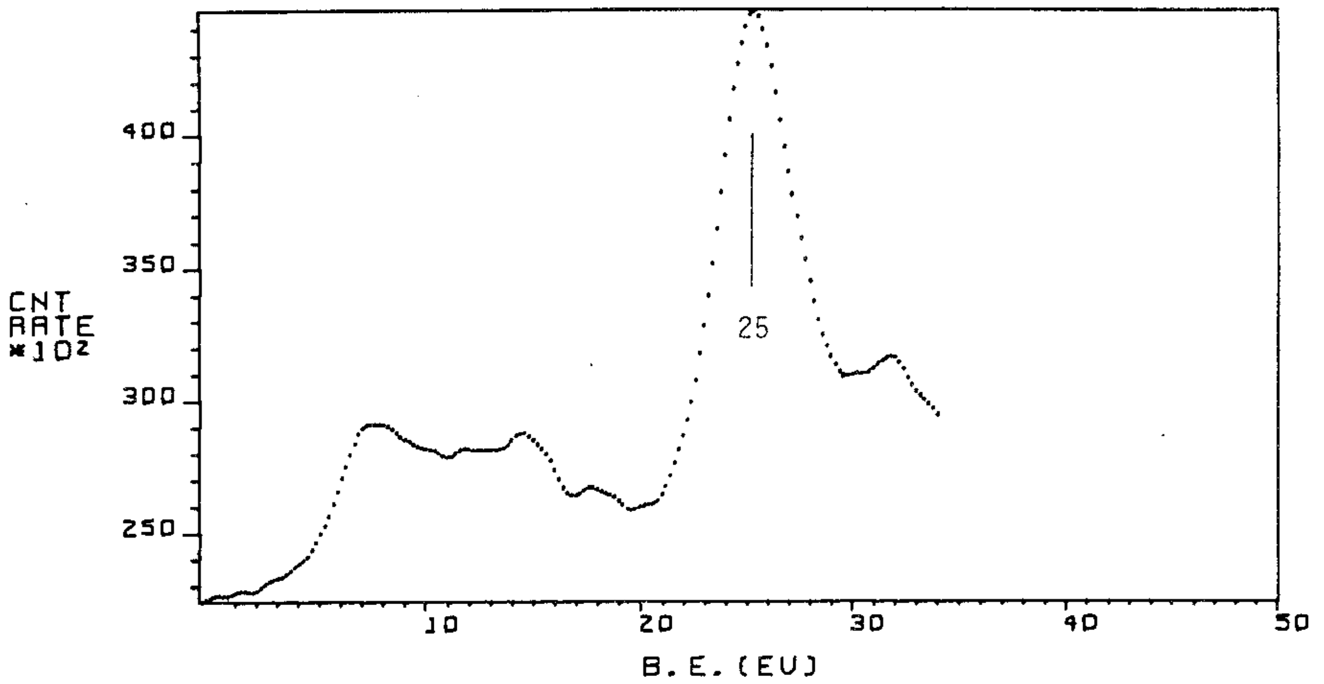

Fig. 29 Valence-band XPS spectrum of SiO_2.

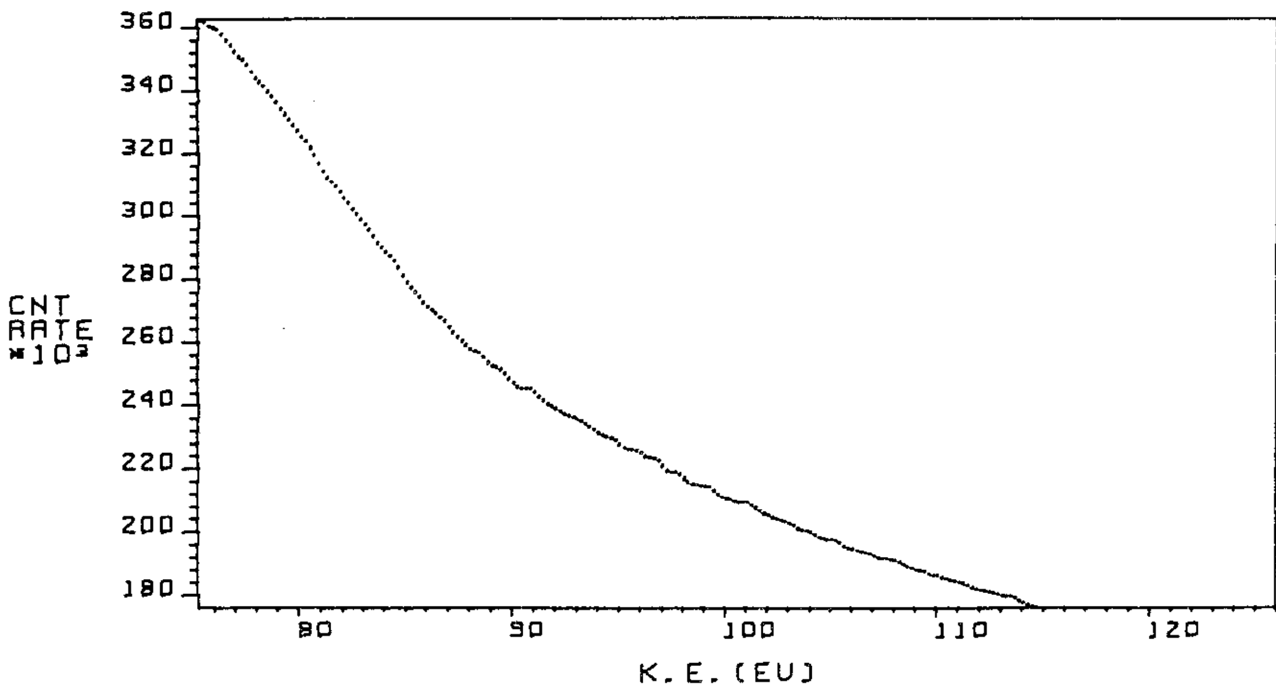

Fig. 30 Si(LVV) XAES spectrum of SiO_2.

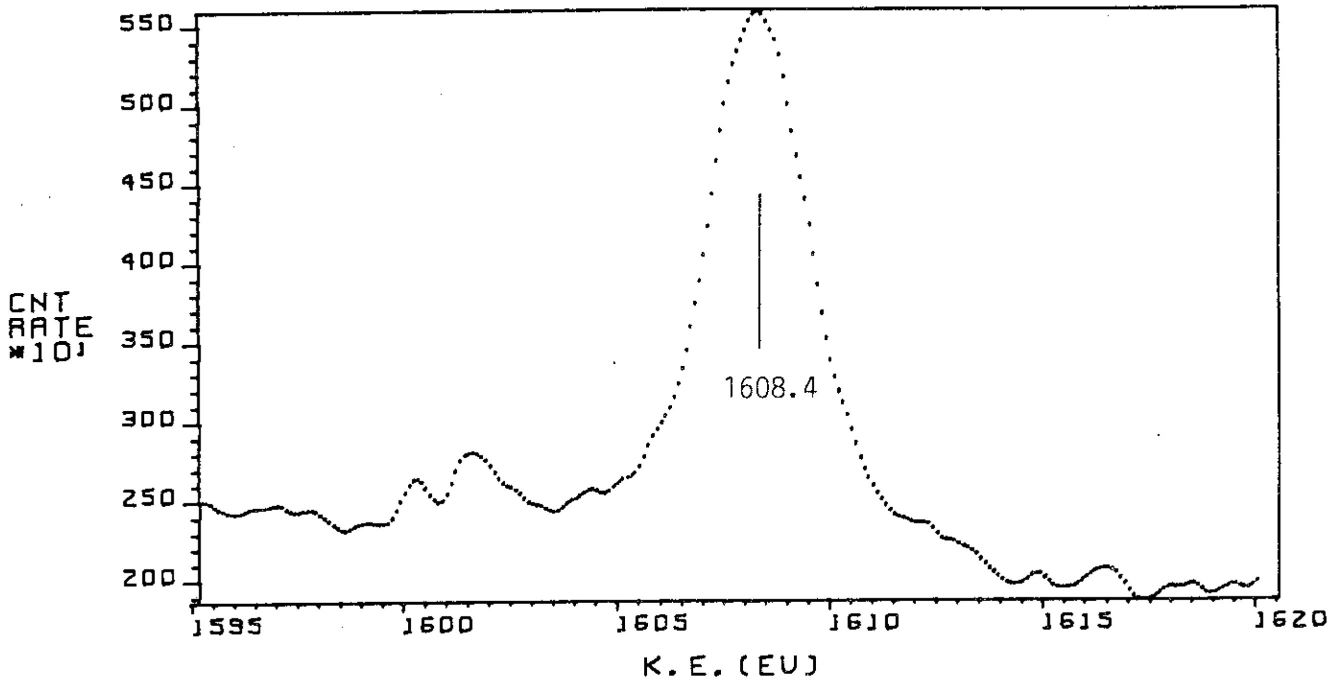

Fig. 31 Si(KLL) XAES spectrum of SiO_2.

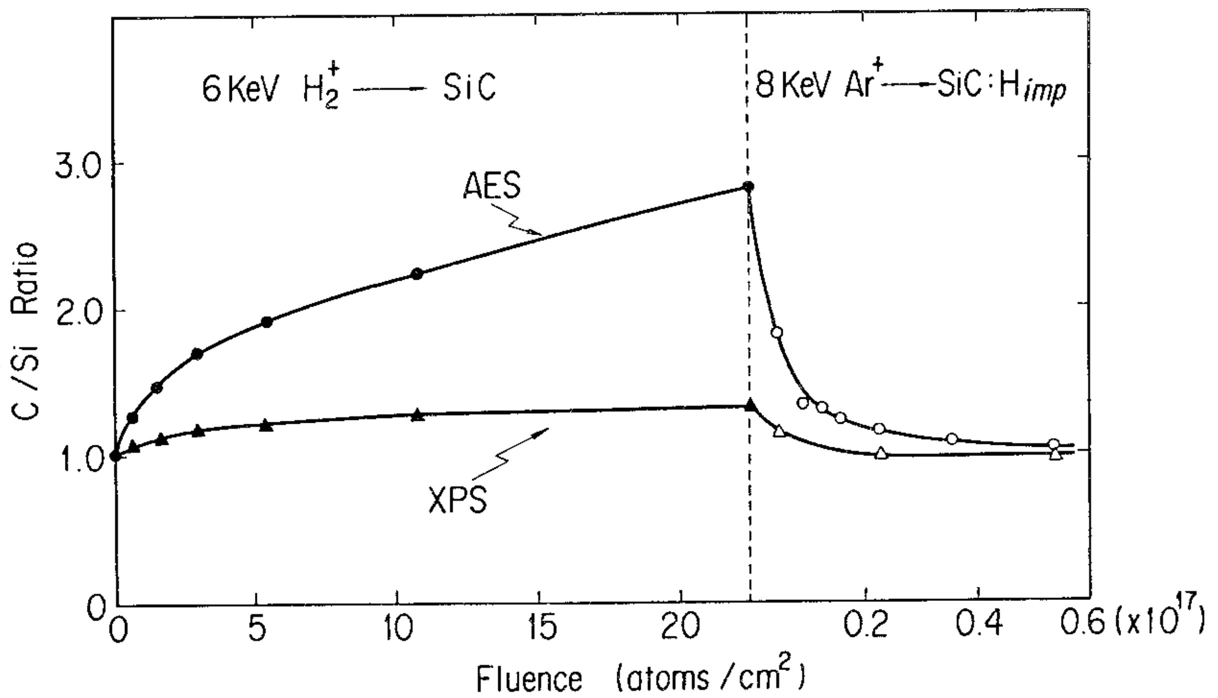

Fig. 32 Changes in C/Si ratio of SiC as functions of hydrogen fluence and Ar^+ ion fluence. AES data were determined from signal ratios of Si(LVV,75 eV)/C(KLL,260 eV).

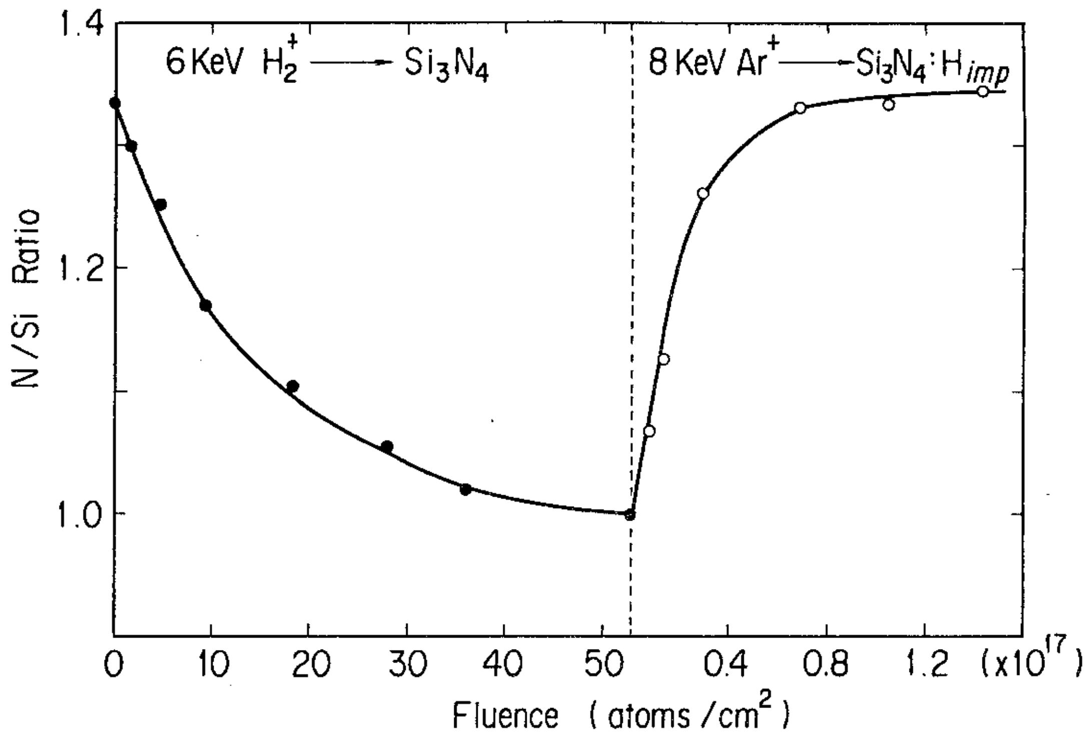

Fig. 33 Changes in N/Si ratio of Si_3N_4 as functions of hydrogen fluence and Ar^+ ion fluence.

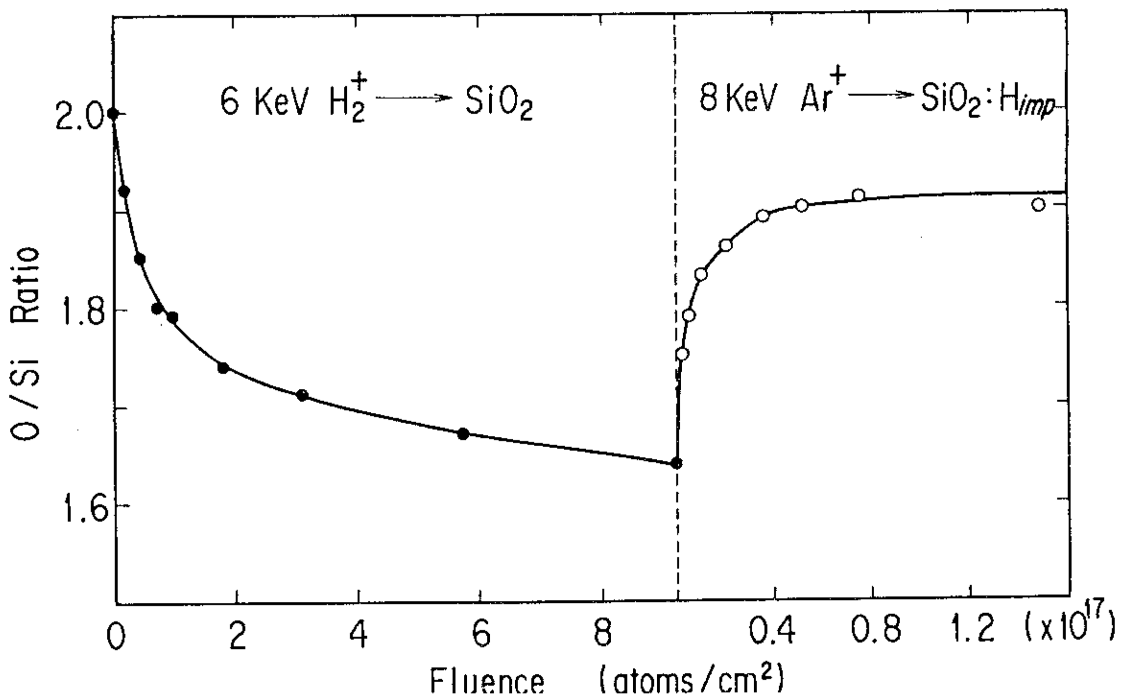

Fig. 34 Changes in O/Si ratio of SiO_2 as functions of hydrogen fluence and Ar^+ ion fluence.

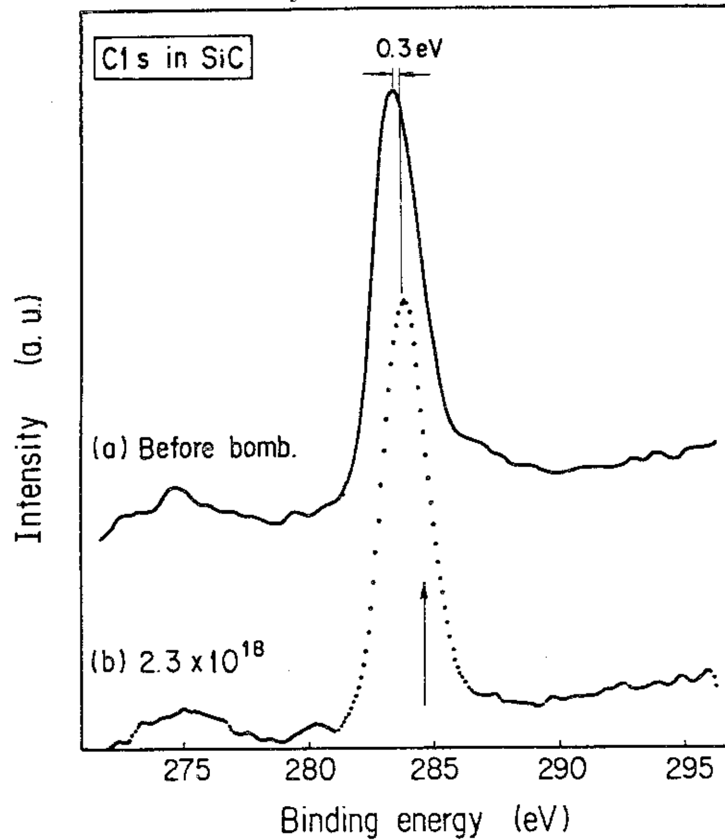

Fig. 35 C1s XPS spectra of SiC before and after 6 keV H_2^+-ion bombardments. An arrow indicates position of C1s line for graphite target bombarded with H_2^+ ions, taken from Fig.36.

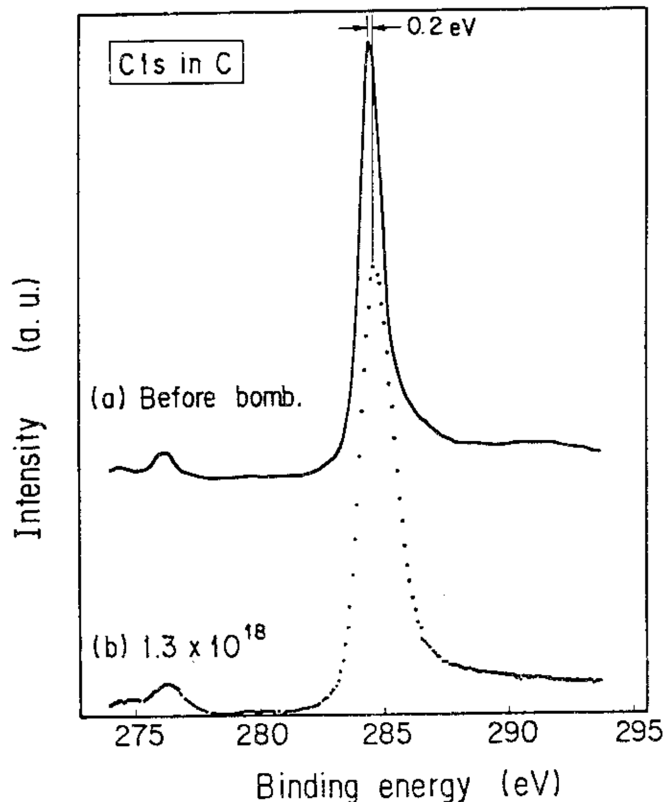

Fig. 36 C1s XPS spectra of graphite before and after 6keV H_2^+-ion bombardments.

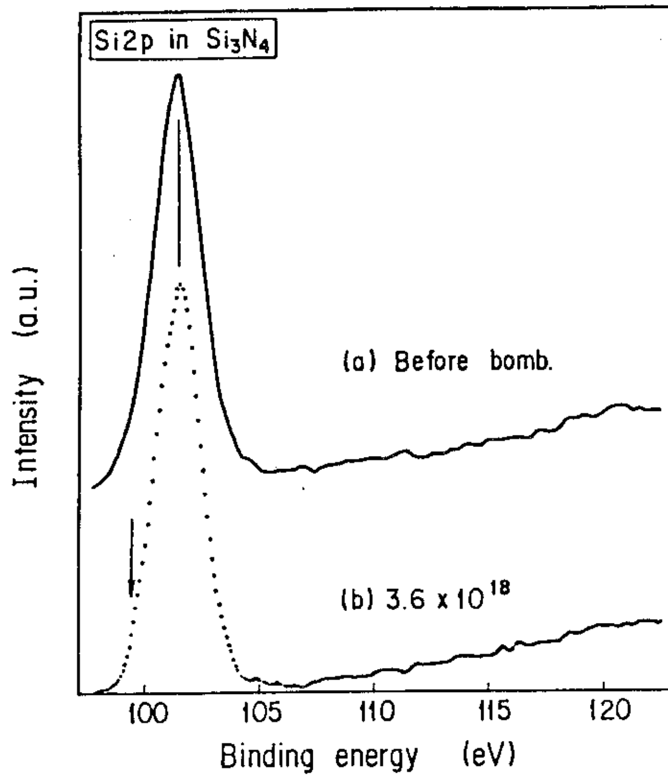

Fig. 37 Si2p XPS spectra of Si_3N_4 before and after 6 keV H_2^+-ion bombardments. An arrow indicates position of Si2p line for Si target bombarded with H_2^+ ions, taken from Fig.39.

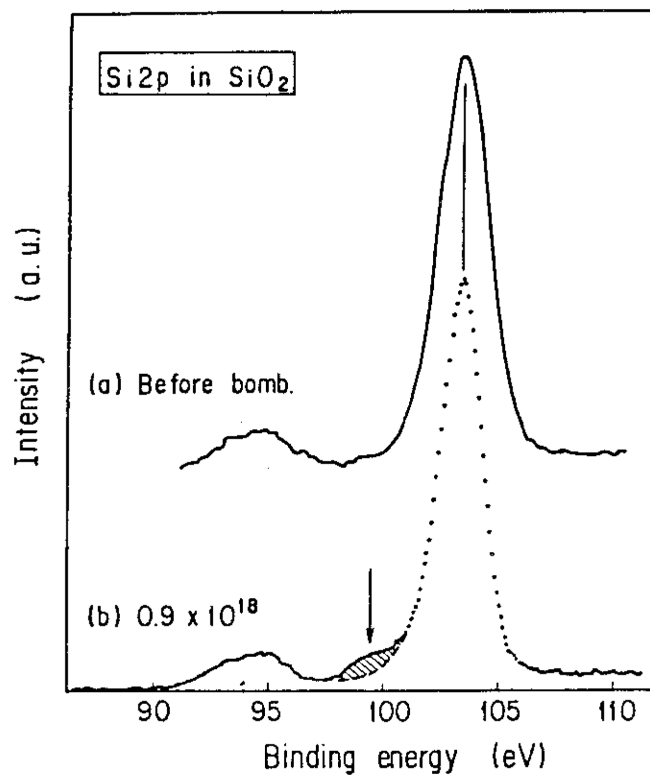

Fig. 38 Si2p XPS spectra of SiO_2 before and after 6 keV H_2^+-ion bombardments. An arrow indicates position of Si2p line for Si target bombarded with H_2^+ ions, taken from Fig.39. Hatched area is attributable to silicon hydride(s).

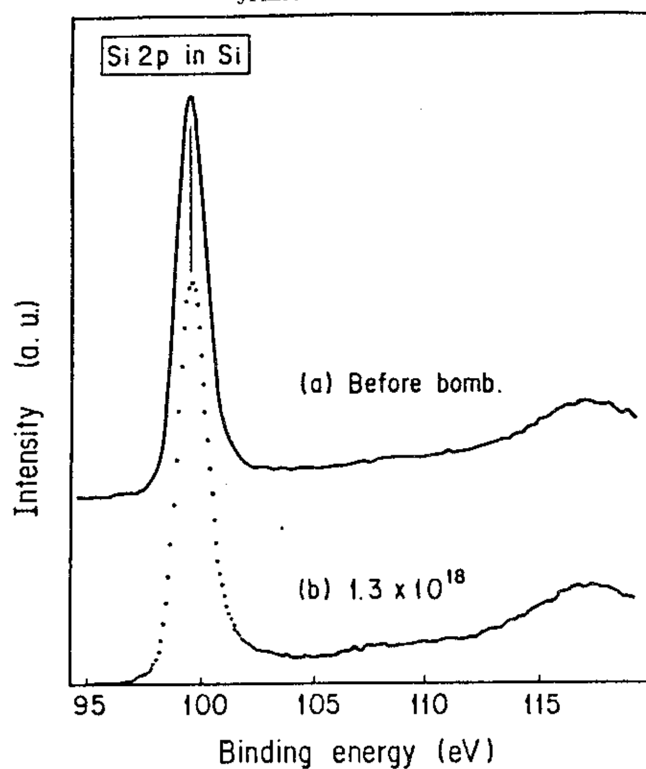

Fig. 39 Si2p XPS spectra of Si before and after 6keV H_2^+-ion bombardments.

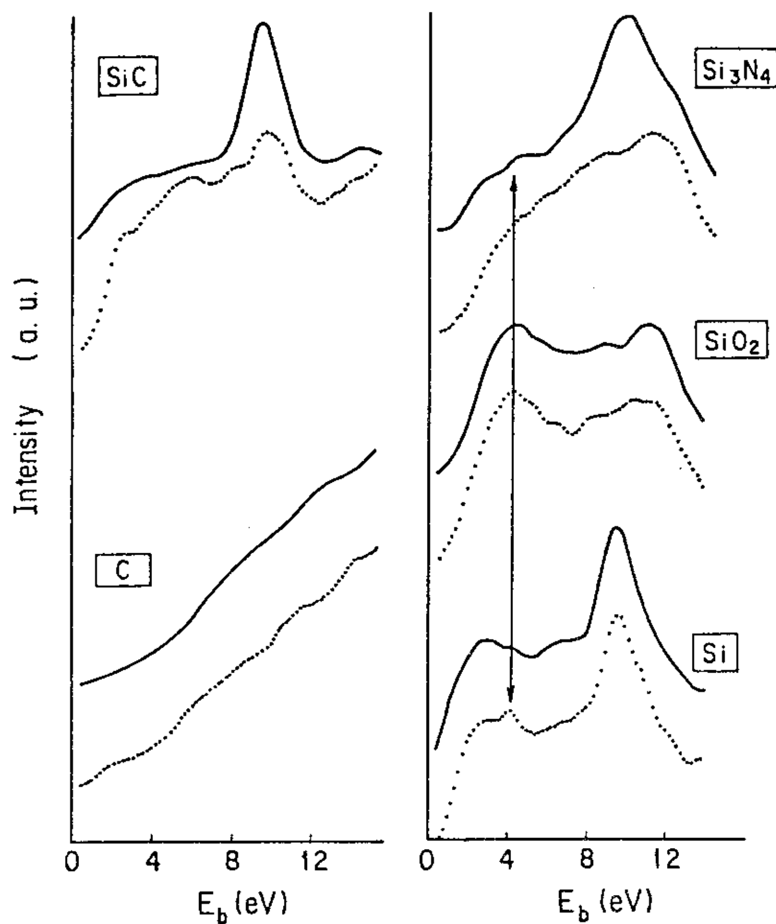

Fig. 40 Valence-band XPS spectra before(—) and after(···) 6 keV H_2^+ -ion bombardments. Note a peak appeared at around 4 eV of Si target. This is attributable to silicon hydride(s).